Study of Phase Transformation and Microstructure of sol-gel prepared-alcohol washed nanostructured Titania

A thesis submitted
in partial fulfillment of the requirements for
the award of degree of

Masters of Technology
In
Metallurgical and Materials Engineering

Submitted by
Gaganjot Singh
Reg. No. 601202004

Under the guidance of
Dr. Poonam Uniyal
Assistant Professor
School of Physics and Materials Science

School of Physics and Materials Science
Thapar University
(Established under section 3 of UGC Act, 1956)
Patiala -147004, INDIA

July 2014

Dedicated to My Late Grandmothers

ਮੇਰੀ ਮਰਹੂਮ ਦਾਦੀ ਅਤੇ ਨਾਨੀ ਨੂੰ ਸਮਰਪਿਤ

Declaration

I hereby declare that the work being presented in this thesis report entitled **"Study of Phase Transformation and Microstructure of sol-gel prepared- alcohol washed nanostructured Titania"** by me in partial fulfillment of the requirements of the award of degree of **Master of Technology** in **Materials Science and Engineering** from **School of Physics and Materials Science**, Thapar University, Patiala is an authentic record of my work carried out under the supervision of **Dr. Poonam Uniyal, Assistant Professor, School of Physics and Materials Science, Thapar University**. The matter presented in this report has not been submitted at any other University institute for the award of Masters of Technology or any other degree.

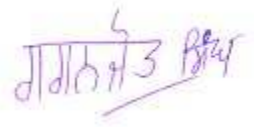

Gaganjot Singh

Registration No: 601202004

I hereby declare that the work being presented in this thesis report entitled **"Study of Phase Transformation and Microstructure of sol-gel prepared-alcohol washed nanostructured Titania"** by **Gaganjot Singh** in partial fulfillment of the requirements of the award of degree of **Master of Technology** in **Materials Science and Engineering** in the **School of Physics and Materials Science, Thapar University,** Patiala is a record of candidate's own work carried out under my supervision. To the best of my knowledge, the content of this thesis does not form a basis for the award of any other degree.

(Poonam)

Poonam Uniyal
Assistant professor
School of physics and Materials science
Thapar University, Patiala

(Countersigned by)

( )

Kulvir Singh
Professor & Head
School of Physics and Materials science
Thapar University, Patiala

( )

S.K. Mohapatra
Dean of Academic Affairs
Thapar University, Patiala

Acknowledgements

To begin with, I would like to express my sincere gratitude to my Supervisor Dr. Poonam Uniyal, *Assistant Professor, School of Physics and Materials Science, Thapar University, Patiala* for her untiring and continuous guidance throughout my entire candidature. Her advice along with constructive and critical evaluations helped me in invoking further thinking in my research area and successful completion of my studies. I would like to express my heartfelt gratitude to her for introducing me to my current research area and guiding and supporting me throughout my research. I would also take this opportunity to thank Dr. Kulvir Singh, *Professor and Head, School of Physics and Materials Science, Thapar University, Patiala* for providing me with the opportunity and invaluable advice in further enriching my interest in materials research.

I thank Dr. B. N. Chudasama, *Assistant Professor and in-charge, Sophisticated Lab, School of Physics and Materials Science, Thapar University, Patiala* for the access to TGA-DSC thermal analyzer and UV-Vis spectrophotometer for sample characterization during my research. Also, I would like to thank Mr. Anil Saini and Mr. Shiv Kumar of *Institute Instrumentation Centre, Indian Institute of Technology, Roorkee* for allowing me to use FE-SEM and TGA-DSC facility for my research. I thank Mr. M. Aggarwal and Mr. Ghanshyam Maurya of *Sophisticated Analytical Instrumentation Laboratory, Thapar University, Patiala* for their help. I also thank Dr. N. K. Verma, *Senior Professor and in-charge Nanomaterials Lab, School of Physics and Materials Science, Thapar University, Patiala* for access to high temperature furnace.

I am very grateful to Ms. Manpreet Kaur (research scholar) for her outmost help through valuable guidance during experiment. I would also like to express my sincere gratitude to Ms. Samita Thakur, Mr. Satwinder Singh and Ms. Sakshi Gupta for making me part of healthy discussions and for helping me with my doubts. I also thank Mr. Gaurav Singla, Mr. Paramjyot Jha, Ms. Chandani Khurana, Ms. Parveer Kaur, Ms. Pooja Singla, Ms. Purnima Sharma, Ms. Navjot Dhindsa, Ms. Geetanjali Dhir, Mrs. Kamaldeep and Mr. Jaspal Singh for their timely helps. I wish to sincerely thank our lab officers Mr. Jant Singh and Mr. Purshotam Singh.

I wish to express my deep gratitude to my family and my friends (Mr. Bharat Bhushan, Mr. Pritampal Singh, Mr. Hitesh Kumar, Ms. Deepshikha Shekhawat, Mr. Amit Sharma, Mr.

Gaurav Kalia, Mr. Kripal Singh, Mr. Mahesh Kumar, Mr. Savidh Khan and Mr. Vinoth Kumar) for their whole-hearted and unconditional support throughout my research.

Finally, I would like to acknowledge the financial support provided by School of Physics and Materials science, Thapar University, Patiala, and Ministry of Human Resource Development (TEQIP scheme) in the form of research grant and teaching assistant scholarship.

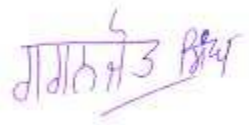

Date: 15-07-2014 **Gaganjot Singh**

Contents

List of figures

List of tables

Abstract

Undoped titanium dioxide was prepared by the means of sol gel technique. Washing of the sol (i.e. either by water or by alcohol) was taken as initial varying input. Powder was synthesized by the hydrolysis of water with the Titanium Isopropoxide in the presence of 2-propanol. As-prepared samples were heat treated at different temperatures ranging from 450° C to 750° C, with the motive to study the effect of different washing treatment on the anatase to rutile phase transformation temperature and the microstructure. Samples were characterized by X-ray diffraction technique (XRD), TGA / DSC, UV-Vis spectroscopy (DRS) and FE-SEM. For water washed samples, anatase to rutile transformation temperature was obtained as 693°C, whereas for alcohol rinsed samples this temperature comes out as 777 °C. Apart from this, micrographs obtained from FE-SEM showed complete densification and exaggerated particle growth in the water washed samples, on the other hand alcohol washed samples showed some small amount of porosity with relatively lower particle size. This behavior of alcohol washed samples had been attributed to 'critical-particle- nuclei-theory' as discussed in detail here in this report.

Chapter: 1 Introduction

1. 1Overview to nanomaterials

Nanomaterials is a class of materials that takes materials science-based approach on nanotechnology. It studies materials with morphological features on the nanoscale and especially those that have special properties stemming from their nanoscale dimensions. Nanoscale is usually defined as smaller than a one thousandth of a micrometer in at least one dimension [1].

Properties corresponding to the nanoscale dimensions of the materials are of great interest these days. In nanomaterials, the ratio of the surface atoms to the total atoms is very large as compared to its counterpart bulk materials. Materials with this large ratio show different properties than their bulk materials. Some of its examples are like change in the color of the bulk gold from bright yellowish to red (at nano level), opaque bulk materials turn to transparent nanoparticles, nano metal oxides exhibit better catalyst properties, conductors may turn to insulator or vice versa at nano scale etc. Also their optical properties, e.g. fluorescence, become a function of the particle diameter. This effect does not come into play by going from macro to micro dimensions. Nanotubes, nanodots, nanofibers, nanowires are some of the possible morphologies that can be obtained at nano level. Some Industries like electronics, catalyst, solid oxide fuel cell, pharmaceuticals are having wide applications of nanomaterials.

For nano materials, as the characteristic length of the microstructure goes down to 1 – 100 nm generally, it becomes comparable with the critical length scale of the physical phenomenon, resulting in 'size – shape effect' leading to drastic change in the properties. Apart from that very high surface to volume fraction makes nanoparticles very reactive due to very high surface energy, due to which these particles undergo reactions to keep its surface energy low. The transitions from microparticles to nanoparticles can lead to a number of changes in physical properties. The major factors in this are the increase in the ratio of the surface area to volume and the size of the particles moving into the realm where quantum effects predominate. Important ways in which nanoscale materials may differ from macro scale materials:

a) Quantum confinement
b) Greater surface area to volume ratio [2].

A certain number of physical properties also alter with the change from macroscopic to nano-scopic system. Novel mechanical properties of nanomaterials are a subject of nano mechanics research. When brought into nano from a bulk material, nanoparticles can strongly influence the mechanical properties of the material, like stiffness or elasticity. For example, traditional polymers can be reinforced by nanoparticles resulting in novel materials which can be used as lightweight replacements for metals. Such nano technologically enhanced materials may enable a weight reduction accompanied by an increase in stability and improved functionality. Catalytic activities also reveal new behavior in the interaction with biomaterials. This ability of the nanoparticles can be exploited by using nano catalyst or photocatalyst. Titanium dioxide has been widely used and studied for its application as a photocatalyst, catalyst support and gas separating membranes.

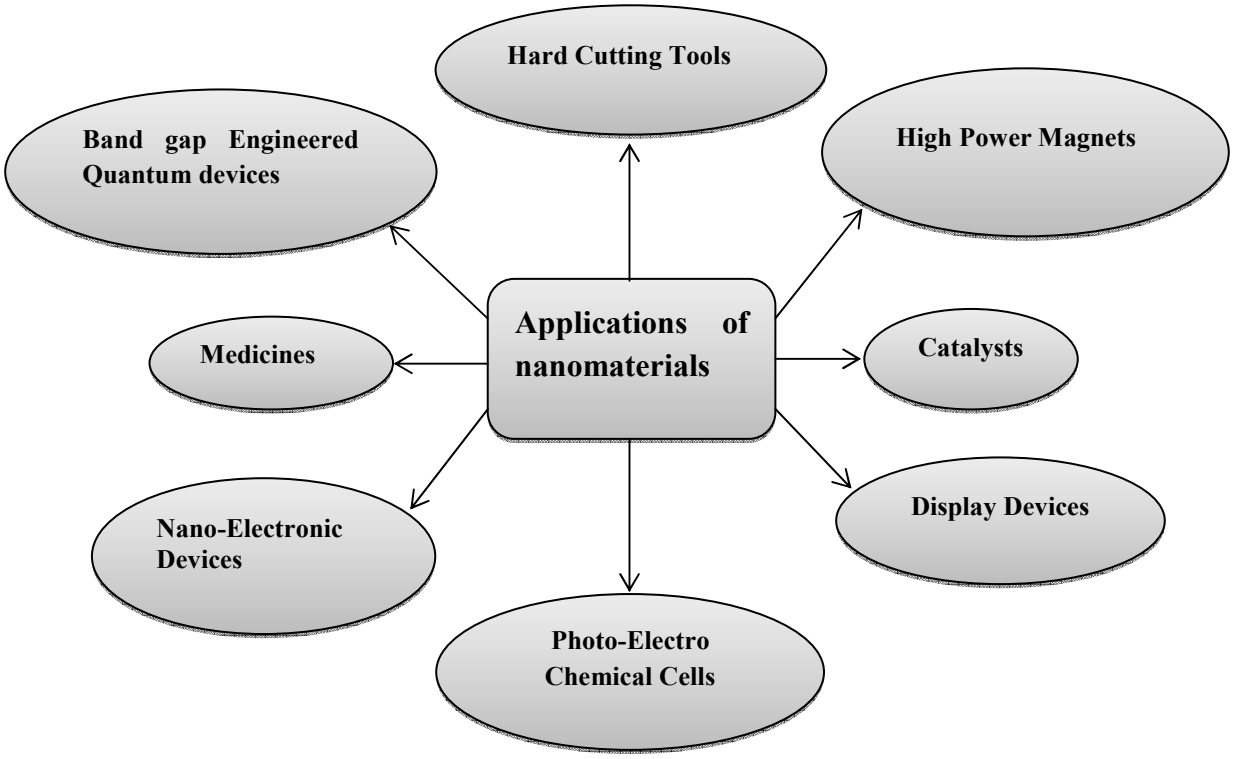

Figure 1. 1General application of Nanomaterials

1. 2Titanium Dioxide

Titanium Dioxide, most commonly known as Titania or Titanium (IV) Oxide is the naturally oxide of Titanium having chemical formula TiO_2. Titanium is the ninth most abundant element in the earth's crust. Titanium dioxide is a white solid inorganic substance that is thermally stable, non-flammable, poorly soluble, and not classified as hazardous according to the

United Nations' (UN) Globally Harmonized System of Classification and Labeling of Chemicals (GHS). Titanium Dioxide mainly occurs in the form of: anatase, rutile and brookite, while rutile being the most thermodynamically stable form.

1.2. 1TiO_2 applications

Now days, titanium dioxide (TiO_2) has widely gained a great deal of attention because of its chemical stability, non-toxicity, low cost and other advantageous properties. Therefore it has been used in worldwide applications such as photovoltaic cells, photocatalysis, environmental purification, photoinduced superhydrophilicity as well as an ingredient in a pigment. With respect to photocatalysis, TiO_2 is close to being an ideal photocatalyst due to its properties as mentioned above. Generally, both anatase and rutile are used as photocatalysts and some research stated that anatase had higher photo activity than rutile. There are some studies which claimed that mixture phases between anatase and rutile provided higher efficiency than the pure phase [3]. This could be the effect of several factors such as specific surface areas, crystallite sizes, and pore size distribution as well as preparation methods. In photocatalytic reactions, TiO_2 can degrade not only organic compounds such as hydrocarbons, chlorinated compounds and nitrogen- or sulfur containing compounds but also inorganic compounds such as nitrogen oxide species (NOx).

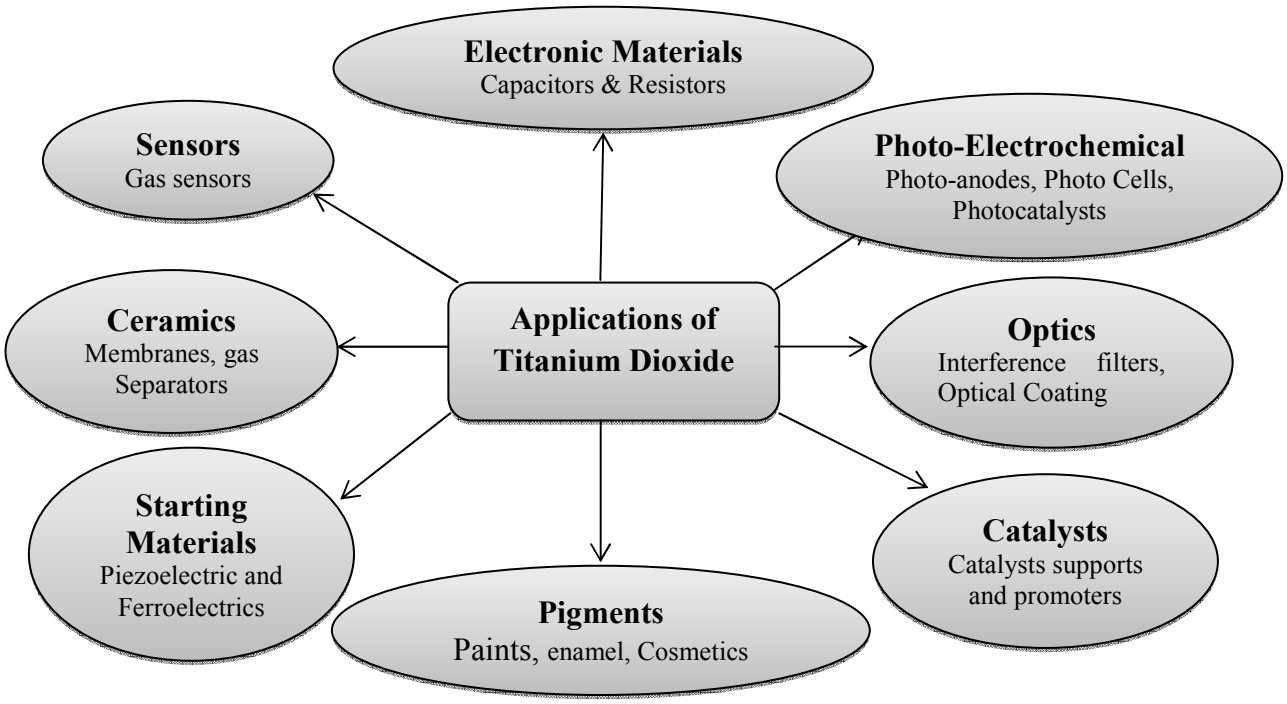

Figure 1. 2Flow chart showing applications of Titanium dioxide.

Overall, photocatalytic reactions can be generally summarized as displayed in figures 1.3 and 1.4. Detail of some of the important application is given as under:

i. Pigments:

It is the one of the most important application of the Titanium Dioxide powder, as it provides whiteness and non-transparency to some of the products like plastics, coatings, paints, ink, paper, food and cosmetics products. Properties like high refractive index and bright white make it as an effective option as an effective opacifier for pigments.

ii. Sensors

In the reducing atmospheres Titania tends to loose oxygen and become sub-stoichiometric. It is well known that reducing gases to be detected remove some of the adsorbed oxygen and modulate the height of the potential barriers, thus changing the overall conductivity and creating the sensor signal. Among the metal oxides that undergo appreciable change in electrical conductivity when exposed to a gas atmosphere TiO_2 is the most commonly used.

iii. Photocatalytic Activity of Titanium Dioxide

The term 'Photocatalysis' can be defined as *a catalytic reaction in which the catalyst utilizes light for reaction kinetics*. In general, *photocatalysis is a reaction which uses photo energy to activate a substance which modifies the rate (generally accelerate) of chemical reaction without its direct involvement in the reaction*. After Fujishima and Honda discovered the photocatalytic splitting of water with the help of TiO_2 electrode, a new age of research started in the field of heterogeneous photocatalysis. Soon after that the semiconductors like TiO_2, ZnO, ZnS and CdS etc. were studied for their applicability as a catalyst.

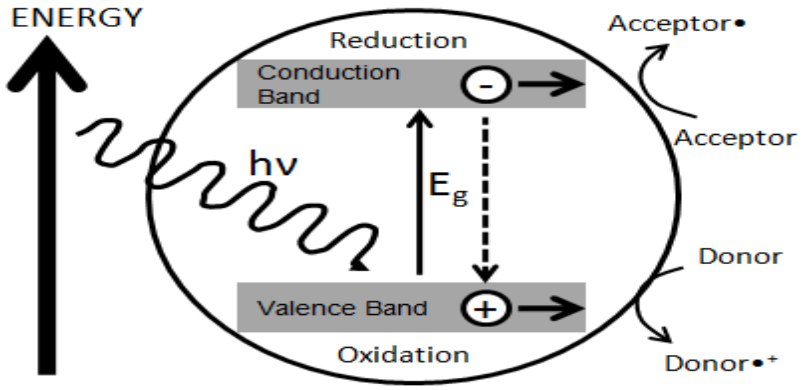

Figure 1. 3Working of a photocatalyst

Chlorophyll in plants is also a kind photocatalyst. Photocatalysis is analogous to photosynthesis; in which chlorophyll captures the sunlight to in order to convert water and carbon dioxide into oxygen and glucose. Similarly photocatalysis produces strong oxidation agent to breakdown any organic matter to carbon dioxide and water in the presence of photocatalyst, light and water. Photocatalysis reaction starts with electron-hole pair generation after bandgap excitation. When a photocatalyst is illuminated by light with energy equal to or greater than band-gap energy, the valence band electrons can be excited to the conduction band, leaving a positive hole in the valence band:

$$\text{Photocatalyst} \xrightarrow{h\nu} e_{CB}^{-} + h_{VB}^{+} \qquad (1)$$

The electron-hole pairs produced can recombine, giving the input energy as heat, with no chemical effect. However, if the electrons (and holes) migrate to the surface of the semiconductor without recombination, they can participate in various oxidation and reduction reactions with adsorbed species such as water, oxygen, and other organic or inorganic species. These oxidation and reduction reactions are the basic mechanisms of photocatalytic water/air remediation and photocatalytic hydrogen production, respectively.

The work of ***Fujishima and Honda*** on the photocatalytic splitting of water in year 1972 opened the field of research. Since then, a lot of research has been done for the utilization of TiO_2 in the area of energy and the environment [4]. A lot of work has been done on the air-water de-contamination. TiO_2 is regarded as the most efficient and environmentally favorable photocatalyst, and it has been most widely used for photo degradation of various pollutants. TiO_2 photocatalysts can also be used to kill bacteria. The strong oxidizing power of illuminated TiO_2 can be used to kill tumor cells in cancer treatment.

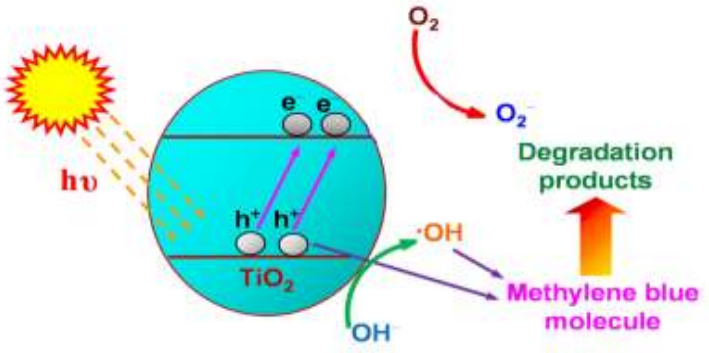

Figure 1. 4Working of TiO_2 as a photocatalyst

The principle of the TiO_2 photocatalytic reaction is straightforward; upon absorption of photons with energy larger than the band gap of TiO_2; electrons are excited from the valence band to the conduction band, creating electron-hole pairs. These charge carriers migrate to the surface and react with the chemicals adsorbed on the surface to decompose these chemicals. This photo-decomposition process usually involves one or more radicals or intermediate species such as $^{\cdot}OH$, O^{2-} or H_2O_2 which play important roles in the photocatalytic reaction mechanisms. The photocatalytic activity of TiO_2 is largely controlled by:

1. The light absorption properties, e.g., light absorption spectrum and coefficient,
2. Reduction and oxidation rates on the surface by the electron and hole,
3. And the electron-hole recombination rate. Also the rate of adsorption of the organic compounds on the surface of TiO_2 semiconductor plays important role in its photocatalytic activity.

1.2. 2Properties of Titanium Dioxide

1.2.2. 1Structural properties of Titanium Dioxide

Naturally, Titanium dioxide exists in three main polymorphic forms: rutile, anatase and brookite. In the past, rutile and anatase have shown photocatalytic activity whereas brookite is photocatalytically inactive. Thermodynamically, rutile is the most stable phase of TiO_2 as compared with other polymorphs like anatase and brookite. Both anatase and rutile possess distorted octahedron class of TiO_6. Six octahedrons of O^{2-} ions surround the Ti^{4+} ions, with each oxygen ion surrounded by three Ti ions. Difference between the structures of the two phases is due to the distortion of the each octahedron and different octahedral chains assembly pattern [5].

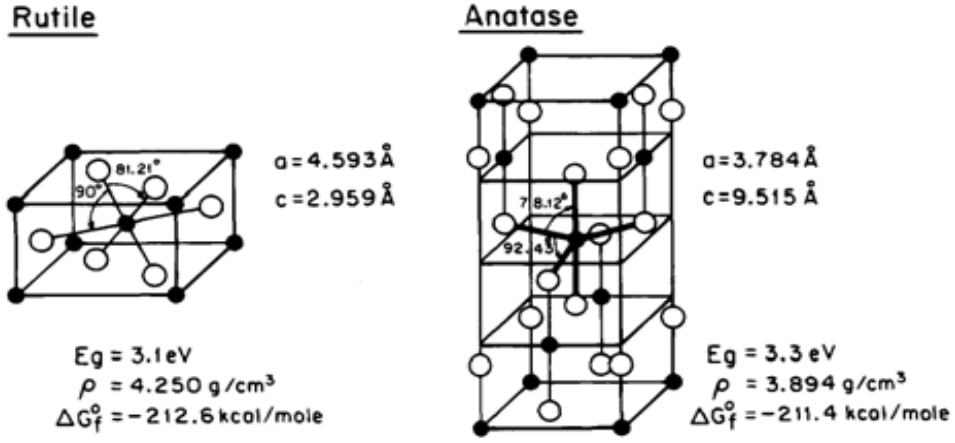

Figure 1. 5Lattice structure of rutile and anatase TiO_2[6]

In case of rutile, slight orthorhombic distortion is there due to which stretching beyond the cubic shape is found, whereas in case of anatase there is less orthorhombic symmetry due to more cubic distortion as compared to rutile. The lattice structure of rutile and anatase are shown above in the figure. Moreover, rutile is the most stable phase of titanium dioxide while anatase and brookite are metastable phases. The metastable structures are almost as stable as rutile at normal pressure and temperature because of small difference in the Gibb's free energy (4-20 kJ/mol) between three phases.

The third form of TiO_2, brookite, shown in Figure, has more complicated structure. The interatomic distance and the O-Ti-O bond angle are similar to those of rutile and anatase phases. The main difference is that there are six different Ti-O bonds ranging from 1.87 to 2.0Å. Accordingly, here are 12 different bonds from 77º to 105º. In contrast, there are only two kinds of Ti-O bonds and O-Ti-O bond angles in rutile and anatase [7].

Due to the difference in the crystal structure of the rutile and anatase, the difference in the electronic structure can be seen which leads to the difference in the band gaps of the two polymorphs. With different band gaps both polymorph exhibits different photocatalytic activity.. Regarding the band gap energy, 3.26 eV (~380 nm) is the band gap energy of anatase and in rutile 3.05 eV (~406 nm) is its energy. Other crystal properties of all three forms of TiO_2 are shown in Table 1.

Table 1. 1TiO_2 crystal structure data [7]

Crystal Structure	System	Lattice parameters (nm)			Lattice Volume (nm^3)	Density (Kg/m^3)	Ti-O bond length (Å)	O-Ti-O bond angles	Band Gap (eV)
		a	B	c					
Anatase	Tetragonal	0.3733	0.3733	0.937	0.13625	3830	1.937 1.965	77.7 º 92.6 º	3.26
Rutile	Tetragonal	0.4584	0.4584	0.2953	0.06207	4240	1.949 1.980	81.2 º 90.0 º	3.05
Brookite	Orthorhombic	0.5436	0.9166	0.5134	0.25738	4170	1.87 2.04	77.0 º 105 º	----

1.2.2.2Thermodynamic behavior of TiO_2

In the various methods leading to the synthesis of TiO_2, anatase is the initial crystalline TiO_2 phase formed generally. If we see from the structural point of view, this is due to the greater ease in arranging of the short-range ordered TiO_6 octahedran into long-range ordered anatase structure relative to rutile. Also, from a thermodynamic perspective, due to the lower surface free energy of anatase, in spite of the lower Gibbs free energy of rutile, the more rapid recrystallization of anatase happens. That is, the crystallization of anatase is favored by higher surface free energy of the rutile. At all temperatures and pressures, rutile is most stable and has lowest Gibbs free energy than all other polymorphs of titanium dioxide. On heating, along with the particle coarsening following transformations also occurs: anatase to brookite to rutile, brookite to anatase to rutile, anatase to rutile, and brookite to rutile.

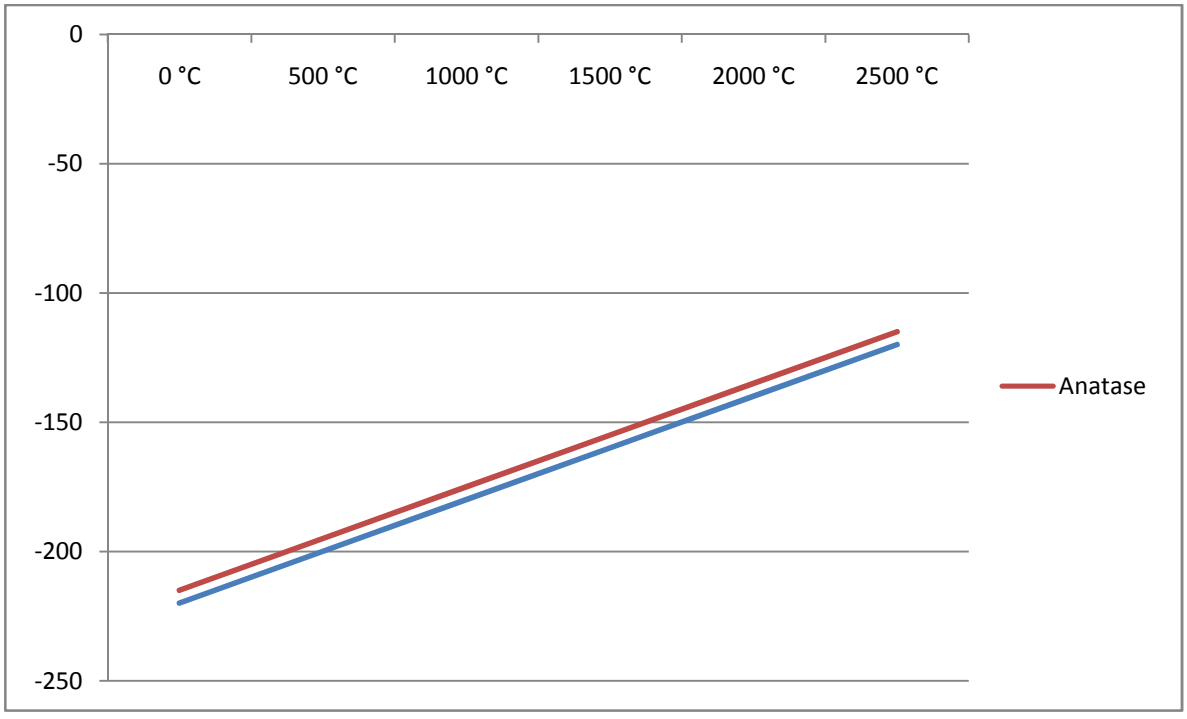

Figure 1. 6Plot of Gibbs free energy (kJ/Mol) [along Y - axis] of anatase and rutile versus temperature (K) [along X - axis] [8]

These transformation sequences imply very closely balanced energetics as a function of particle size. The transformation to rutile is irreversible. The study of the anatase to rutile transformation from the above transformations is of importance, as anatase possesses better photocatalytic properties, so the understanding of this transformation is necessary.

1. 3Anatase to rutile transformation

The anatase to rutile transition, sometimes referred to as the ART, is a nucleation and growth process. The kinetics of this transition is dependent on variables such as:

- Impurities,
- Morphology,
- Sample preparation method,
- Heat flow conditions, etc.

In the absence of impurities, dopants, secondary phases, or other types of contamination, rutile forms as fine laths with the product phase's (100) planes parallel to the (112) planes of the parent anatase. In pure anatase, rutile may nucleate at (112) twin interfaces in anatase as these sites are structurally similar to rutile. *The anatase to rutile transformation is reconstructive, which means that the transformation involves the breaking and reforming of bonds*. This is in contrast to a displacive transformation, in which the original bonds are distorted but retained. The reconstructive anatase to rutile transformation involves a contraction of the c-axis and an overall volume contraction of 8%.

Control of the conditions that affect the kinetics to control the anatase to rutile phase transformation is of considerable interest because for high-temperature processes and applications, such as gas sensors and porous gas separation membranes [9], where the phase transformation may occur, thereby altering the properties and performance of these devices. Therefore, an understanding of the stabilities of the TiO_2 polymorphs, the kinetics of their phase transformation, and the processes involved in controlling them is essential to the ability to obtain single-phase or multiphase microstructures. These issues are critical to the long-term consistency of devices, where retention of anatase or a multiphase microstructure may not be possible, thereby potentially requiring processing designed to produce single phase rutile.

Similarly, limitations in temperature while desiring a specific polymorph, such as rutile, may require manipulation of the materials and processing conditions so as to enhance the direction formation of rutile. The generation of the phases of TiO_2 depends significantly on the synthesis parameters, which in turn affect the product. The kinetics of these processes is typically considered in terms of temperature and time. In terms of the former, pure bulk anatase is considered widely to begin to transform irreversibly to rutile in air at 600° C; however, the reported transition temperatures vary in the range 450 - 1200° C.

The anatase to rutile transformation is not instantaneous; it is time dependent. Consequently, the kinetics of the phase transformation can be interpreted in terms of all of the factors that influence the requisite temperature–time conditions. These parameters for un-doped anatase are: Particle size, particle shape (aspect ratio), surface area, atmosphere, and volume of sample, nature of sample container, heating rate, impurities (from raw materials and container) and measurement technique.

1. 4Design strategies for developing thermally stable nanostructured Titania

1.4. 1Need for the design

As titanium dioxide is having anatase and rutile as its primary forms, anatase shows better photocatalytic activity as compared to its counterpart, which has been reported by a number of researchers in the past, whereas rutile shows better optical and electronic properties. Here our area of concern is the photocatalytic activity of titanium dioxide or its application as a stable catalyst support. At high temperature, the metastable anatase phase starts transforming to the thermodynamically stable rutile phase. As mentioned earlier, anatase possess better photocatalytic behavior than rutile, so it becomes our prime necessity to either retard the phase transformation rate or to completely eliminate the transformation. Apart from this, generally the metastable to stable type of transformation are followed by sharp decrease in surface area and porosity, which are one of the primary aspects that must be kept in mind while designing a catalyst. The rate and exact temperature of the phase transformation depends on the numerous things like primary particle size, pH value of solution, drying and washing temperature, packing of primary factors, reaction condition etc. [10]. Also the electron – hole pair recombination time is also a problem, which has to be increased for better photocatalytic activity. In order to of tackle the above problems related to the photocatalyst, a fine engineered material should be prepared for enhanced catalytic properties.

1.4. 2Different designs strategies for developing thermally stable Titania are characterized as under:

1) Physical Methods
   - Freeze drying method
   - Alcohol washing method
   - TiO_2matrix based Composite

2) Chemical Method

- Doping
    - Cationic doping
    - Anionic doping

Chapter: 2 Literature Review

Titanium Dioxide is the oxide form of the titanium, which is being used in the many applications like catalyst, pigments, paints, sunscreen, food preservation, hydrogen production etc. [11-16]. These applications make it a prime research topic. Since the experimental results put up by Fujishima and Honda in the year 1972 regarding the photocatalytic splitting of water using TiO_2 electrode, the TiO_2 has become one of the prime research fields. From the early study it has been concluded that anatase is photocatalytically more active polymorph of Titania than rutile [17]. Also, some other studies brought up that high porosity and surface area are highly desirable for better catalytic activity [18-19]. Better permeability has been reported earlier for the extraporous separative membranes [20]. From the above literature it can be concluded that study of the phase transformation of anatase with change in temperature is important for synthesizing thermally stable Titania, which fulfill the requirements of a good catalyst. After reviewing the literature, we pointed out some following reasons for the ART phase transformation.

2. 1Effect of Impurities/Dopants

The influence of impurities on the nucleation and growth of rutile from anatase is that they create oxygen vacancies, such as the addition of acceptor dopants (ions with a lower valence that Ti^{4+}) and use of reducing atmospheres accelerate the anatase-rutile transformation [21]. An increase in the concentration of oxygen vacancies reduces the strain energy that must be overcome before the rearrangement of the Ti-O octahedran can occur, and that cations with a valence less than that of Titania (4+) will increase the concentration of oxygen vacancies, due to the necessity for charge balance. This defect chemical reaction shows that for every mole of impurity introduced into the system, one mole of doubly ionized oxygen vacancies are created for charge compensation. The monovalent ions are more effective than divalent or trivalent ions. When ions of lower valency replace Ti^{4+} in the lattice, anion vacancies that compensate for the different charge disrupt the lattice [22]. Thus, more oxygen vacancies would need to be created for monovalent dopants compared to divalent or trivalent. This effect is offset to some extent by the greater ease with which higher-charged and consequently smaller ions can fit into the lattice. It has also been reported that the effectiveness of dopants increased with their concentration, up to about 1mole %. When rutile nucleates more readily, it has more time to grow and agglomerate than it otherwise would. Agglomerate size is also affected by sintering temperature and time, as

well as potential segregation of additives [22]. But on the contrary it had been reported that the presence of all dopants, both donor and acceptor cations as well as anion dopants, inhibits the anatase-rutile transformation by stabilizing the anatase phase [23]. Additives with a higher charge seemed to stabilize the anatase phase more strongly than those with a lower charge. Tin oxide has been used previously as a dopant in Titania systems [24]. The coordination number of tin and titanium are the same, and the cation to anion radius ratios are nearly identical, being 0.51 and 0.49, respectively.

2. 2Effect of Atmosphere

Several researchers have studied the effects of different atmospheres on the anatase-rutile phase transformation, with somewhat conflicting results. The reducing atmospheres such as steam, a H_2/N_2mixture (5%-95%, respectively), and vacuum (10^{-1}Pa) yield the formation of large aggregates of rutile [22]. It was also found that the use of the H_2/N_2atmosphere yielded up to 97% rutile with an aggregate size of 3.5μm, while the vacuum and steam atmospheres yielded between 20% and 30% rutile with an aggregate size of 2μm. Similar reactions in air yielded less than 10% rutile. A nearly linear relationship between % rutile in the samples and aggregate size as measured by scanning electron microscopy, such that aggregate size increased with an increasing amount of rutile.The effect of **air / Ar** and **Cl_2 / Ar** atmospheres on the anatase-rutile transformation, calcined in the different atmospheres for a range of times[25]. Here, chlorine assists both vapor mass transport, which is a possible mechanism for nucleation on the solid surface, and oxygen vacancy formation, which assists nucleation and growth in the bulk material.

2. 3Effect of Precursor

Study of the effects of preparation method and titanium precursor on the resulting Titania crystal structure has not been comprehensive. The effects of sulfate and chloride solutions suggested that although the initially dried products were always amorphous, the first crystalline forms present varied with preparation method and precursor solution[26]. Samples originating from sulfate solutions always gave the anatase structure, while samples produced from the boiling of chloride solutions always gave the rutile structure. Other methods of synthesis such as hydrolysis of phosphate solutions or hydrolysis at room temperature gave either the anatase structure or a

mixture of both the anatase and the rutile structure. An amorphous phase always existed prior to the crystalline phase, on the use of Titanium Isopropoxide as a precursor.

2. 4Effect of Particle Size on Phase Transformations

There are two main effects of particle size on phase transformations that will be discussed in this section. Garvie *et al.* first explained the "critical particle theory" with reference to the zirconia system [27]. Thistheory has been applied to the Titania system by Rao *et al.*[28].

In the zirconia system, which is in many ways analogous to the Titania system, there is a tetragonal to monoclinic phase transformation.

Under the critical nuclei size effect theory, a nucleus will only be stable when it reaches a critical size, 'r_c'. Given that all else is constant, critical nucleus size depends only upon the transitional energies involved, as shown:

$$r_C = \frac{-2g_S}{g_v + g_e} \quad (2)$$

The significant particle-size effect on the anatase-rutile transformation rate in nanocrystalline Titania whereby an increase in reaction rate was associated with a decrease in particle size. Three rate-limiting factors can be offered as explanation, each relating particle size to a change in reaction rate:

i. Potential Nucleation Sites

Due to purely geometrical effects, the overall number of potential surface nucleation sites per unit volume increases with a decrease in particle size. As the number of potential sites per unit volume increases, it would logically follow that the number of surface nuclei increases, increasing the rate of phase transformation.

ii. Driving Force

The driving force for a phase transformation is the difference in free energies between the reactant and product phases. Anatase has a lower surface energy than rutile and therefore would imply that as crystallite size decreases, so does the driving force, which would result in a reduced reaction rate. This is inconsistent with the experimental data provided by Gribb and Banfield and was therefore discounted as a reasonable explanation.

iii. Strain Energy

Since the molar volume of rutile is 8-10% less than that of anatase, there is likely to be strain energy associated with the phase transformation. Because of differences in surface tension and

hydrostatic-like pressure on smaller crystallites, this strain energy may be affected by particle size. As particle size decreases, the surface tension and hydrostatic-like pressures would potentially reduce the strain energy, reducing one of the barriers to transformation.

Furthermore studies had been carried out on the titanium dioxide, anatase to rutile transformation and photo catalytic activity of titanium dioxide. In this chapter we have reviewed the previous literature which laid the foundation for this work. This has helped us to give a better understanding about the topic and also acts as a guideline for our thesis. In this chapter, experimental and theoretical efforts on synthesis process and characterization of Titania and detailed proposed theories for explaining the experimental results have been reviewed and discussed.

In year 1958 **Rao** *et al.* were first to report the transition of anatase to rutile, which occurs below 610°C and the transition was immeasurably slow. Whereas above 730 °C, transition occurred extremely rapidly. They also stated that the conversion was second-order transition [28].

In 1979**George Lager** *et al.* in their paper stated that the TiO_6 octahedra in the three polymorphs of TiO_6 differ with respect to size and distortion at room temperature and pressure. The change in distortion with heating, was measured by the octahedral bond angle variance. These distortions were different for the three polymorphs; the octahedron in brookite came out as less distorted, whereas in anatase there was an increases in distortion and rutile remained effectively unchanged [29].

In the same year **Mitsuhashi** *et al.* proposed the stability sequence for the modifications of $TiO_2$to be rutile >brookite>anatase, which was consistent with the sequence implied by their enthalpy of solution data [30].

In 1993 **Kumar** *et al.* studied the stability of a titania- alumina composite and pointed that main mechanism of porosity and surface area reduction was enhanced sintering occurring during anatase to rutile transformation which was being followed by grain growth. They further proposed that pore growth and porosity reduction can be retarded by retarding anatase crystallite growth or by retarding the phase transformation or both [31]. Same year in another study of unsupported Titania membranes they pointed that Titania membrane precursor xerogel gel layers made from the hydrolysis of Titanium Isopropoxide contained anatase crystals. Also, they concluded that in undoped Titania gel, transformation initiated from dislocations and defects.

They measured the BET surface area to be 165 m^2g^{-1} for as prepared gel dried at 40°C, 30 m^2g^{-1} after heating at 450°C and immeasurable at 500°C [32]. Further extending their study to supported membranes they obtained relatively smaller crystallite size than the crystallite size of unsupported membrane from their previous study (20nm and 70nm for supported and unsupported membranes). They assumed that this behavior was due to the decrease in the driving force for sintering due to the stresses developed during the constrained sintering of the membrane attached to a rigid support. They noted the ART temperature at 850° C [33].

Kumar in 1995 from their study of undoped Titania and titania-alumina composite concluded that primary particle size of anatase was smaller than the critical nuclei size of rutile, which may be the reason behind the high chance of obtaining metastable phase when prepared through sol gel synthesis method. Particle size of the precipitates formed was generally 4 to 10 nm, which was considerably below the critical nuclei size of rutile [34]. In another study of composites, same year, **Kumar** *et al.* reported that there was a possibility of retardation of sintering of the matrix phase because of back stress effects and the influence of rigid second phase network formation. At 800° C they achieved the porosity and surface area of 10 % and $3m^2g^{-1}$ respectively with 9 % of Al_2O_3 as second phase [35].

Kumar *et al.* in the 1998, reported that in case of titania and tin oxide composite that, pure titania transformed to more than 95 % rutile and completely dense with zero porosity at 800° C, whereas samples containing 2.4 mol % of tin oxide retained 70 % of rutile and surface area of $16m^2g^{-1}$ at 750° C and at 800° C retained $8m^2g^{-1}$ of surface area with 100% rutile phase. They concluded that SnO_2 enhanced phase transformation and also retarded densification and particle growth during transformation [36].

Hong et al. in 1998 investigated the effects of alcohol washing on the crystallization behavior of precipitated titanium oxide using FTIR, TGA-DSC, X-Ray diffraction and IR spectroscopy. They observed the crystallization temperature of amorphous precipitates into anatase as 467° for alcohol washed samples as compared to 390°C of water washed. From FTIR the found that alcohol rinsed powder had a dehydration rate much lower than that of non-rinsed powder as the temperature increases. So the presence of oxy-alkoxides in alcohol rinsed samples decreased the dehydration rate which in turn retarded the crystallization of anatase structure [37].

Banfield *et al.* in 2000 proposed that the energies of the three polymorphs (of TiO_2) are size dependents and are very close that they can be reversed by small difference in surface

energy. They also stated that if particles size of the three nanocrystalline polymorphs can be obtained equal, anatase can be the most thermodynamically stable at sizes less than 11 nm, brookite between 11 and 35 nm and rutile is stable at sizes greater than 35 nm. Their samples transformed from anatase to brookite and / or rutile and then brookite to further rutile. They calculated the activation energy for anatase to brookite transformation to be 11.90 kJ-mol^{-1} and for brookite to rutile as 163.8 kJ-mol^{-1}[38].

Gray *et al.* in their study confirmed the intermediacy of Ti^{4+}sites in the phase transformation from anatase to rutile. Also, they demonstrated that tetrahedral Ti^{4+}sites contribute to the increased photocatalytic activity of mixed phase material relative to the pure phase anatase [39].

The work of **Kumar** *et al.* in year 2009 of alcohol washing of Titania can be summarized by saying that replacement of water with lower surface tension pore fluid like 2-propanol had enhanced the thermal stability of sol-gel derived Titania. Lower packing density was achieved by alcohol washed Titania which exhibit slower phase transformation and particle growth. Alcohol washed gels also had retained higher surface area and porosity. For alcohol washed and water washed gels ART transformation temperature was obtained as 853°C and 816°C respectively. In addition their results pointed at the importance of critical-nuclei-size-effect in the metastable to stable phase transformation of nanostructured anatase Titania [40].

Okubo *et al.* in 2010 studied the influence of the particle size and packing of the anatase crystallite on the phase stability of nanostructured Titania. Anatase gels with different particle packing were synthesized by stabilization induced through peptization of the sol. In case of well packed Titania, initial size of anatase primary particles does not influence the phase transformation whereas loosely packed gels showed a strong initial anatase primary particle size dependence on the phase transformation behavior [41].

Marta *et al.* in 2013 found that there was an increase in anatase to rutile transformation degree with temperature and calcination time. At higher temperature the higher values of anatase to rutile transformation rate constants were achieved. Modifiers like boron, tin and antimony didn't show any influence on the ART temperature, with Zinc increased degree of transformation and zirconium, cerium limited the degree of transformation [42].

Carlo *et al.* in 2013 proposed the light induced phase transition of TiO_2 nanoparticles from anatase to rutile structure depending on the surrounding environment and the

transition being accomplished under oxygen poor conditions. The transition mechanism was interpreted in the framework of oxygen adsorption and desorption phenomena with the involvement of surface oxygen vacancies. It was shown that the observed phase transition was not thermally driven because the local temperature of the nanoparticles during irradiation was of about 370 K (estimated through the Stokes to anti-Stokes Raman peaks ratio). On the contrary, the phase transition is initiated by intra-gap irradiation, that acts as TiO_2 surface sensitizer, promoting the activation of the surface and the nucleation of rutile crystallites starting from two activated anatase neighboring nanoparticles [43].

Mattsson *et al.* reported that phase stability, surface chemical and photocatalytic properties of Zr and Y co-doped anatase TiO_2nanoparticles prepared by homogenous hydrolysis methods using urea as precipitating agent were performed. It was showed that Y and Zr ions replace Ti ions in the anatase TiO_2structures up to a critical total dopant concentration of approximately 13 wt%. The co-doped particles show increased phase stability as compared to pure anatase TiO_2nanoparticles. The anatase to rutile phase transformation was preceded by cation segregation. Co-doping modified the optical absorption edge with a resulting attenuation of the Urbach tail. The bandgap was slightly blue-shifted at high doping concentrations, and red shifted at lower doping concentrations. A decrease in photocatalytic activity was observed in the results. This decrease in photo-degradation rate with increasing dopant concentration was explained by the adsorbate structure, which is controlled by the acidity of the surface [44].

In the experiment performed by **Noguchi** *et al.*TiO_2films were deposited by reactive-mode sputtering, followed by a thicker growth layer by radical-assisted sputtering. The effect of the structure of the nucleation layer on the density, crystallinity and photocatalytic properties of the final films was investigated. The kinetic energy of sputtered particles was found to affect the amount of three-dimensional island growth that occurred. The optimum structure was found to be one in which few particles have undergone growth. This had not only produced a dense final structure, but the crystallinity is improved due to chemical annealing by radicals during the second growth step, leading to a film with excellent photocatalytic properties. This indicates the importance of an initial structure that facilitates absorption and diffusion of radicals[45].

An ordered meso structured TiO_2 thin films were obtained by **Wang** *et al.* in 2014 through a method that combined sol−gel with evaporation-induced self-assembly (EISA). It was found that the calcination temperature, as well as the type of block copolymer, could vary the

TiO_2 mesoporous structure. It was also found that varying the mass ratio of templating agent to inorganic precursor could adjust the pore size of mesoporous TiO_2. The samples calcined at 450−500°C, which had a higher specific surface area and larger pore size, exhibited higher photocatalyzed destruction capability of Methylene Blue[46].

2. 5 Motivation

After reviewing the above mentioned literature; we come to this conclusion that, the conditions which control or affect the kinetics of anatase to rutile phase transformation are of distinction interest. Applications like gas sensors and porous gas separation membranes or photocatalysis, where the transformation of phase can happen, the properties of the system changes. Therefore, the stability of the TiO_2 polymorphs is needed to obtain single-phase or multiphase microstructures for desired applications. From literature reviews we come to the conclusion that a very less work has been done on the physical methods to avoid or retard the phase transformation. Even smaller work has been done on the 'alcohol washing' of the Titania. The result presented the different literature of 'alcohol washing' method are also contradictory with each other. So we take this opportunity to study the effect of alcohol washing on the phase transformation of Titania.

Chapter: 3 Experimental Process and Characterization

Experimental Techniques

In this chapter, we are going to discuss briefly the details of the sample preparation technique and the characterization techniques followed by us during the course of investigation.

3. 1Sample Preparation Technique

In order to synthesis nano sized particles at lower temperature, sol gel method of synthesis was followed. Sol-gel is a wet chemical process in which a solution of metal-organic compounds is subjected to hydrolysis and condensation reactions leading to a M−O−M gel structure (M=metal, O=oxygen). If the chemical reactions are controlled properly, the solution will become a structured liquid containing a matrix of metal-organic chains. When dried, the evaporation of solvents leads to an amorphous structure called a gel, which is formed by the cross-linking of metal-organic groups altogether [47].A sol-gel is a colloidal solution of metal-organic [M $(OR)_{n-1}$]molecules which are linked in to an M −O−M polymeric network. The solution is formed by controlled hydrolysis and condensation reactions of metal alkoxides. As follows:

$$\boldsymbol{M(OR)_n + H_2O \rightarrow HO - M(OR)_{n-1} + ROH} \quad (3)$$

$$\boldsymbol{(OR)_{n-1}\, M - OR + HO - M(OR)_{n-1} \rightarrow (OR)_{n-1}M - O - M(OR)_{n-1} + ROH} \quad (4)$$

$$\boldsymbol{HO - M(OR)_{n-1} + HO - M(OR)_{n-1} \rightarrow (OR)_{n-1}M - O - M(OR)_{n-1} + H2O} \quad (5)$$

Where M can be any metal such as Ti etc., and R denotes an alkyl radical. The eq. 11 stands for hydrolysis, whereas eq. 12 and 13 stands for condensation reactions. The hydrolysis consists of replacing one OR group of alkoxide with a hydroxyl ion (OH), releasing an alcohol molecule in the process. Condensation is the reaction between two partially hydrolyzed molecules[HO - M $(OR)_{n-1}$]or one partially hydrolyzed molecule and one alkoxide molecule [M $(OR)_n$]to form a) M −O−M molecule with a [$(OR)_{n-1}$]attached to each metal atom. By definition, condensation liberates either an alcohol or a water molecule, depending on the initial compounds [47].

The hydrolysis and condensation reactions are reversible. The speed of reaction depends on the concentration of the initial compounds and can be altered by other reactants which inhibit

the gelation process. If the hydrolysis/condensation reaction reaches equilibrium with its reverse reaction, the solution will never gel in a sealed container. Such a solution is called a stable sol-gel.

By varying the amount of water/alcohol, it is possible to control the speed of each reaction and shift the equilibrium in either direction. If one were to remove alcohol from a stable sol-gel, this would decrease the speed of the reverse reactions, and would shift the equilibrium toward hydrolysis and condensation. If enough alcohol is removed from the solution, it will eventually gel [48]. Chelating compounds can also modify the gelation [49]. Moreover, the ambient temperature also plays important roles in the final properties. S. Doeuff *et al.* has published a comprehensive study of the various process variables and their effect on the TiO_2 chemical structure [50].

Titania Preparation:

Powder Titania (TiO_2) was prepared by the hydrolysis of alkoxide of titanium i.e. Titanium Isopropoxide **[**Ti (OCH $(CH_3)_2)_4$**]**. Titanium Isopropoxide of 52.64 mL (0.18 mol) was mixed with 445.20 mL of 2 – Propanol. As prepared solution was added drop - wise by the means of a burette into the 350.00 mL of distilled water under constant vigorous stirring at 298 K. A milky white solution with oxy - titanium hydroxide precipitates was obtained. Precipitates in the form of gel were obtained by centrifugation at 5000 rpm for 10 minutes. Gel was divided into two equal parts. One part was washed five times by distilled water and other part by 2 – propanol (alcohol) for five times. Water washed and Alcohol washed gels were put into the oven at 100° C for 24 hours. Dried gels were grounded with the help of agate mortar. These dried powders were calcined at 450° C, 500° C, 600° C, 700° C, and 750° C. A schematic view of synthesis route is shown in the form of flow chart here. Here the chemical reactions taking place during the experiment are given as under:

$$\boldsymbol{Ti\,[OCH(CH_3)_2]_4 + 4\,H_2O \rightarrow Ti\,(OH)_4 + 4\,(OCH\;(CH_3)_2\;OH} \quad (6)$$

$$\boldsymbol{Ti\,(OH)_4 \rightarrow TiO_2\;\; nH_2O + (2-n)H_2O} \quad (7)$$

here ‘n’ is the number of water molecule attached to titanium dioxide.

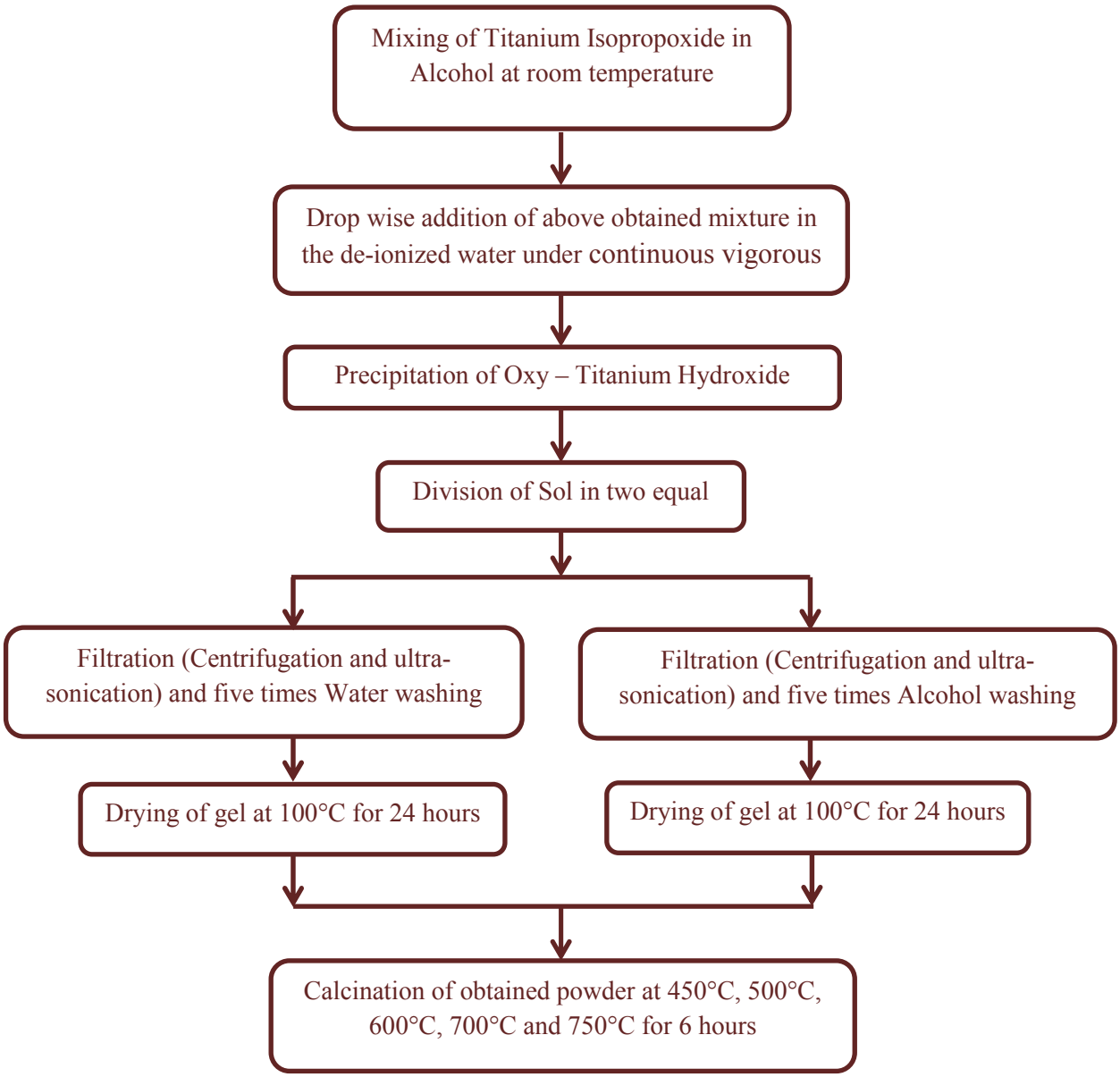

Figure 3.1Flow diagram for synthesis route followed during sample preparation.

3. 2Characterization Techniques

3.2. 1X - Ray diffraction (XRD)

X - Ray diffraction (XRD) is a non-destructive materials characterization technique used mainly for qualitative and quantitative analysis of the ordered materials. X - ray diffraction pattern of a substance is like figure prints of that very material. We can determine the crystal structure, lattice parameters, crystallite size, residual stress, strain etc. We used copper Kα source having wavelength 1.5406 Å for powder diffraction x-ray diffraction. X - ray diffraction pattern was obtained between the 2θ values of 20° to 80° having scanning step size of 0.013°(along 2θ).

3.2.1. 1Generation / Production of X – Rays

X – Rays can be produced by the bombardment of a metal target usually copper with the beam of electrons emitted from hot filament plate usually made of tungsten. The electrons coming from the hot filaments will ionize the K shell electrons of the copper target. Ionization will make the electron to vacate its position. Vacancy of electron in the K shell will make the electron from the L and M shell to drop down in order to fill the vacant site. This dropping of electron from L and M will give rise to the K_{α} and K_{β}. Also continuous spectrum is produced due to the rapid deceleration of the high energy electrons by multiple collisions with the hot filament. This continuous spectrum is also called bremsstrahlung.

3.2.1. 2Interpretation and Calculations

a) Bragg's Law

In a lattice, the atoms are periodically arranged. X – Rays diffracted from crystalline solid makes the constructive interface and thus producing a diffracted beam from these atoms.

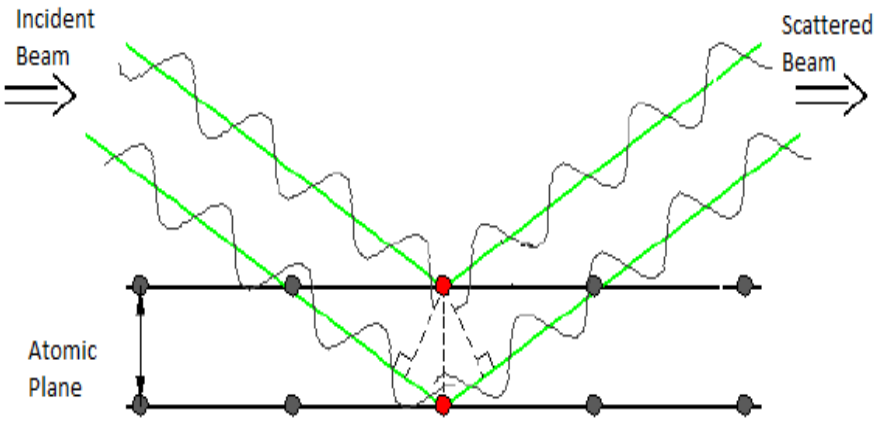

Figure 3.2 Illustration of Bragg's law

William L. Bragg in year 1912 found a predictable relation between different factors, which all are combined in the Bragg's law:

$$n\lambda = 2d \sin \theta \quad (8)$$

Where **n** is an integer, **d** is the inter planner distance in Å, **θ** is the diffraction angle and **λ** is the wavelength of incident x – ray beam in nm.

b) Measurement of crystallite size by using Scherer's formula

Identification of the phase depends mainly on the position of the peaks along the 2θ in the X – ray diffraction graph. IT also depends on the relative intensities of these peaks. Diffraction pattern is affected by the presence of defects such as dislocations, so it is important to take them into consideration. Small crystal size causes peak broadening. The crystallite size (t) can be calculated as function of peak width, peak position and wavelength of x-ray as described by Scherer's formula:

$$t = \frac{0.9\,\lambda}{B\,Cos\theta} \tag{9}$$

3.2. 2Thermal Techniques

3.2.2 1Differential Thermal Analysis

Differential Thermal Analysis or DTA is a technique for thermal analysis, in which the material under study and the reference material undergo similar thermal cycles and the difference between the sample and reference are collected. Graph obtained called DTA curve or thermo gram is plotted with difference in temperature against time or temperature. Sample undergoes some changes due to the effect of applied temperature, which can be either exothermic or endothermic. Differential thermal analysis curve provides information about the various transformations that have taken place like glass transition, crystallization, melting or sublimation. Enthalpy change can be obtained by calculating the area under DTA curve.

a. Interpretation of data:

In principle the onset of the DTA curve gives the starting temperature, but due to location of thermocouples with respect to sample and reference, there can be some temperature lag. To get rid of this difference the system must be calibrate with the materials of known melting point.

1. Melting:

Change of material from solid state to the liquid state is accompanied by the endothermic change in the enthalpy. The DTA curve corresponding to the melting point depends on the purity and the crystallinity of the sample, rate of change of temperature and the thermal resistance between the sample pan and sample holder.

2. Crystallization:

When an amorphous material transform into crystalline solid state, an exothermic change in the enthalpy can be obtained at the DTA curve. The position of the crystallization curve in the Thermo gram is determined by the heating rate. Crystallization temperature can be determined in a same manner as that of melting point.

3.2.2 2Thermal Gravimetric Analysis:

Thermal gravimetric analysis or TG is the measure of change in the mass of the sample with respect to temperature and time. Many transformations involve change in mass like as in case of sublimation, evaporation, decomposition or other chemical reactions etc. The selection of the environment for example air or inert environment (N_2, He, Ar etc.) is also a crucial factor for the results. The rate of heat transfer to the sample depends on the rate of the gas flow.

a) Principle:

- Under a controlled temperature program, the change in mass for the subjected sample is studied.
- Usually temperature program is a linear increase in the temperature but isothermal studies can be carried out when changes in sample mass with time are followed.
- TGA is inherently quantitative, and therefore an extremely powerful thermal technique, but gives no direct chemical information. The ability to analyze the volatile products during a weight loss is of great value.

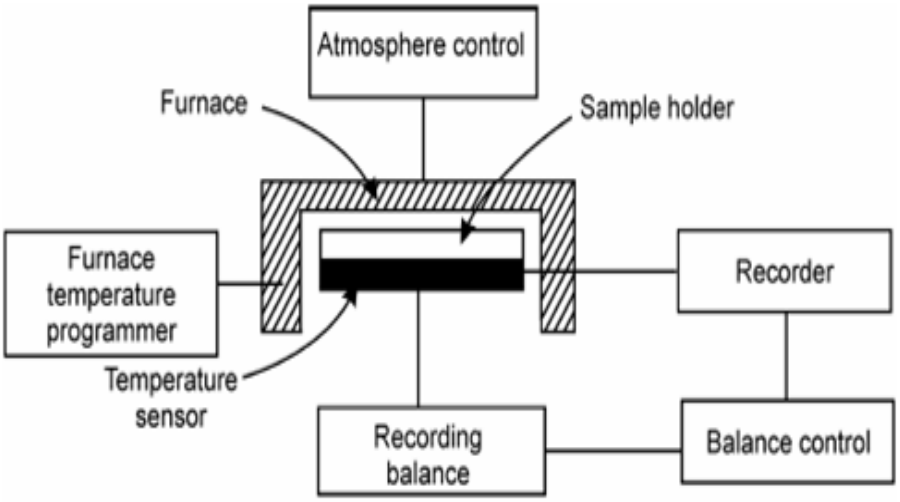

Figure 3.3 Basic construction of a TGA/DSC apparatus

b) Instrumentation:

- Thermo-balance

  Usually the balance having sensitivity up to one microgram and overall weighing capacity of few millimeters is used.
- Temperature programmer

  A typical operating range for the furnace is ambient to 1500°C, with heating rates up to 200°C / min.
- Furnace
- Temperature sensors / Thermocouples
- Sample holder
- An enclosure for required atmosphere

  Reactive or inert

TGA-DSC analyses were carried out using NETZSCH-STA-449F3 thermal analyzer, with heating up to 1000° C at a rate of 10°C / minute in an inert (nitrogen) atmosphere and alumina crucibles.

3.2. 3UV-Vis Spectroscopy:

Band gap measurement is one of the important characterizations in case of photocatalysts, semiconductors, solar materials and other nanomaterials. 'Band gap' can be termed as the difference in the energy levels of valance band and the conduction band or the energy required by an electron to make a jump from valance band to conduction band.

Many molecules absorb the ultraviolet and visible light photons. According to Beer's law this absorbance is directly proportional to the path length b, concentration of the adsorbing species.

$$A = \mathrm{E}bc \tag{10}$$

Where E is the coefficient of absorbance known as absorbtivity.

Every molecule absorbs the photons of a particular wavelength which makes the absorbance spectra fingerprint for that particular molecule. An absorption spectrum will show a number of absorption bands corresponding to structural groups within the molecule.

A. Electronic transitions

The excitation of outer electrons corresponds to the absorption of UV or Visible light. There are three types of electronic transition that are possible here:

1. Transitions involving p, s, and *n* electrons
2. Transitions involving charge-transfer electrons
3. Transitions involving *d* and *f* electrons

When an atom or molecule gets energy from the photon, electrons excites from their ground state to an excited state. In a molecule, rotation and vibration are the only possible movements atoms can possess with respect to each other. These vibrations and rotations also have discrete energy levels, which can be considered as being packed on top of each electronic level.

B. Absorbing species containing p, s, and n electrons

Absorption of ultraviolet and visible radiation in organic molecules is restricted to certain functional groups (chromophores) that contain valence electrons of low excitation energy. The spectrum of a molecule containing these chromophores is complex. This is because the superposition of rotational and vibrational transitions on the electronic transitions gives a combination of overlapping lines. This appears as a continuous absorption band.

Possible electronic transitions of p, s, and *n* electrons are as following:

1. σ to σ^* Transitions
2. n to σ^* Transitions
3. n to Π^* and Π to Π^* Transitions

3.2. 4Field Emission Scanning Electron Microscopy:

This is one of the widely used instruments in material research laboratories. In this technique, electrons are used instead of light waves to see the microstructure of surface of a specimen. However since electrons are excited to high energy (keV), so wavelength of electron waves are quite small and resolution is quitehigh. The electromagnetic lenses used in it are not a part of image formation system, but just helps to focus the electron beam on specimen surface. This gives two of the major benefits of SEM: range of magnification and depth of field in the image, giving three dimensional information of image.

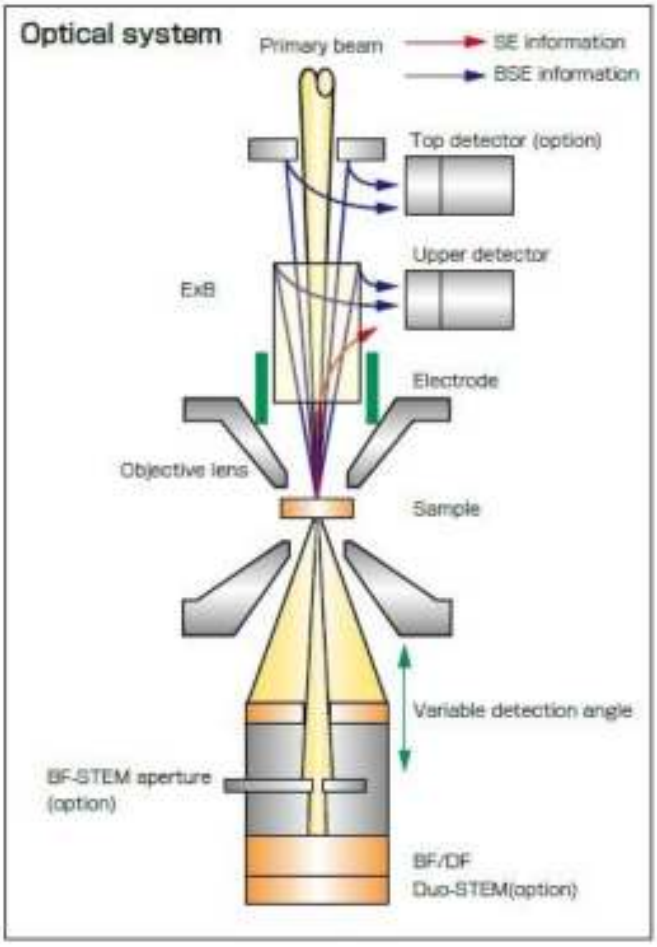

Figure 3.4 Schematic view of FE-SEM apparatus

In a typical SEM, electrons are thermionically emitted from a tungsten or lanthanum hexa-boride (LaB_6) cathode and are accelerated towards an anode; alternatively, electrons can be emitted via field emission (FE). Tungsten is used because it has the highest melting point and lowest vapor pressure of all metals, thereby allowing it to be heated for electron emission. The electron beam, which typically has an energy ranging from a few hundred eV to 100 keV, is focused by one or two condenser lenses into a beam with a very fine focal spot sized 1 nm to 5 nm. The beam passes through pairs of scanning coils in the objective lens, which deflect the beam horizontally and vertically so that it scans in a raster fashion over a rectangular area of the sample surface. When the primary electron beam interacts with the sample, the electrons lose energy by repeated scattering and absorption within a teardrop-shaped volume of the specimen known as the interaction volume, which extends from less than 100 nm to around 5 μm into the surface, The size of the interaction volume depends on the beam accelerating voltage, the atomic

number of the specimen and the specimen's density. The energy exchange between the electron beam and the sample results in the emission of electrons and electromagnetic radiation which can be detected to produce an image, as described below. The most common imaging mode monitors low energy (<50 eV) secondary electrons. Due to their low energy, these electrons originate within a few nanometers from the surface. The electrons are detected by a scintillator-photomultiplier device and the resulting signal is rendered into a two-dimensional intensity distribution that can be viewed and saved as a Digital image. This process relies on a raster-scanned primary beam. The brightness of the signal depends on the number of secondary electrons reaching the detector. If the beam enters the sample perpendicular to the surface, then the activated region is uniform about the axis of the beam and a certain number of electrons “escape" from within the sample. As the angle of incidence increases, the "escape” distance of one side of the beam will decrease, and more secondary electrons will be emitted. Thus steep surfaces and edges tend to be brighter than flat surfaces, which results in images with a well-defined, three-dimensional appearance. Using this technique, resolutions of 1 nm are possible. Backscattered electrons consist of high-energy electrons originating in the electron beam that are reflected or back-scattered out of the specimen interaction volume. Backscattered electrons may be used to detect contrast between areas with different chemical compositions, especially when the average atomic number of the various regions is different, since the brightness of the BSE image tends to increase with the atomic number. Backscattered electrons can also be used to form electron backscatter diffraction (EBSD) image. This image can be used to determine the crystallographic structure of the specimen.There are fewer backscattered electrons emitted from a sample than secondary electrons. The number of backscattered electrons leaving the sample surface upward might be significantly lower than those that follow trajectories toward the sides. Additionally, in contrast with the case with secondary electrons, the collection efficiency of backscattered electrons cannot be significantly improved by a positive bias common onEverhart Thornley detectors. This detector positioned on one side of the sample has low collection efficiency for backscattered electrons due to small acceptance angles. The use of a dedicated backscattered electron detector above the sample in a "doughnut" type arrangement, with the electron beam passing through the hole of the doughnut, greatly increases the solid angle of collection and allows for the detection of more backscattered electrons.

Samples were subjected to high resolution Field Emission - Scanning Electron Microscopyusing

CARL ZEISS- ULTRA PLUS - 55. Samples were observed at the magnifications of 50K to 100K. Samples were coated with gold in order to make them conducting.

Chapter: 4 Results and Discussions

4. 1Results

4.1. 1X-ray powder diffraction (XRD)

Figure 4.1 shows the XRD patterns of water washed TiO_2 samples calcined at different temperatures varying from 450^{o}C to 750 ^{o}C at a step of 100° C. The samples show crystalline phase even at 450° C.

With the increase in calcination temperature all the characteristic peaks of TiO_2 are evident. All the peaks are identified using software X'PERT Hi-score Plus. The characteristic peaks of phases of anatase, brookite and rutile matched with the (01-084-1285), (01-076-1936) and (01-077-0442) JCPDS cards respectively for the Titania at 450°C. Lattice parameters and the d-spacings were calculated by using the combination of following formulas:

$$2d \sin\theta = n\lambda \quad (11)$$

$$\frac{1}{d^2} = \frac{h^2 + k^2}{a^2} + \frac{l^2}{c^2} \quad \text{(For tetragonal system)} \quad (12)$$

$$\frac{1}{d^2} = \frac{h^2}{a^2} + \frac{k^2}{b^2} + \frac{l^2}{c^2} \quad \text{(For Orthorhombic system)} \quad (13)$$

The lattice parameters and d-spacing calculated from the above equations were of the same order as mentioned in the above stated JCPDS standard cards. The hkl values of (101), (211) and (110) belonging to anatase, brookite and rutile phases respectively were used for all the calculations.

The average crystallite sizes were estimated using the Scherrer's formula (Equation 4), where K is the shape factor (it depends on the crystallite type), we have taken K as 0.9 for our calculations, λ is the applied X-ray's wavelength, β is the line broadening at half the maximum intensity in radian for the sample, D is the crystallite size and θ is the Bragg angle:

$$D = \frac{K\lambda}{\beta cos\theta} \quad (14)$$

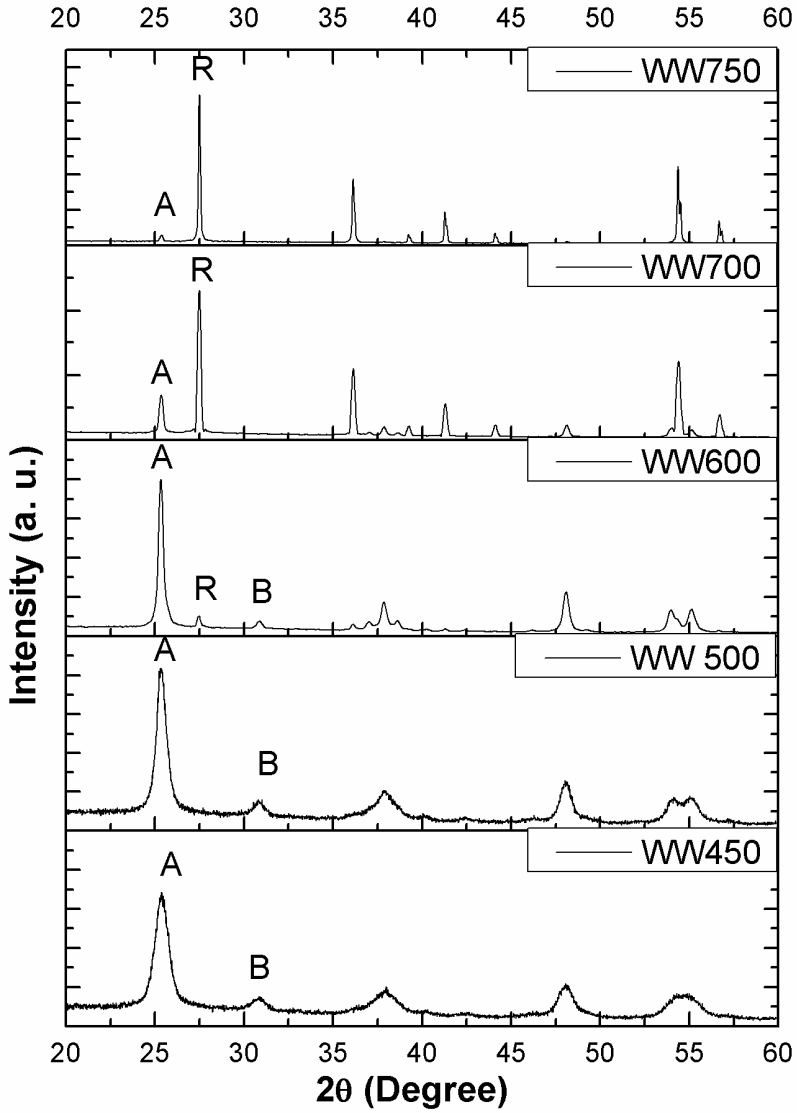

Figure 4. 1XRD pattern for water washed samples calcined at different temperatures.

The weight (W) fraction of each crystal phase was calculated for each sample from the peak area of the anatase (A_A), rutile (A_R) and brookite (A_B) peaks at 25.3° (2θ) (101), 27.5° (110) (2θ) and 30.8° (2θ) (121) respectively. Throughout the calculation some correction factors (k_A, k_B) were applied for each peak area, as follows:

$$W_A = \frac{k_A A_A}{k_A . A_A + A_R + k_B . A_B} \tag{15}$$

$$W_B = \frac{k_B A_B}{k_A . A_A + A_R + k_B . A_B} \quad (16)$$

$$W_R = \frac{A_A}{k_A . A_A + A_R + k_B . A_B} \quad (17)$$

Here A, B, R represents the anatase, brookite and rutile respectively. D_{avg} is the average crystallite size. W_A, W_B, W_R stands for the weight percentage of anatase, brookite, rutile respectively.

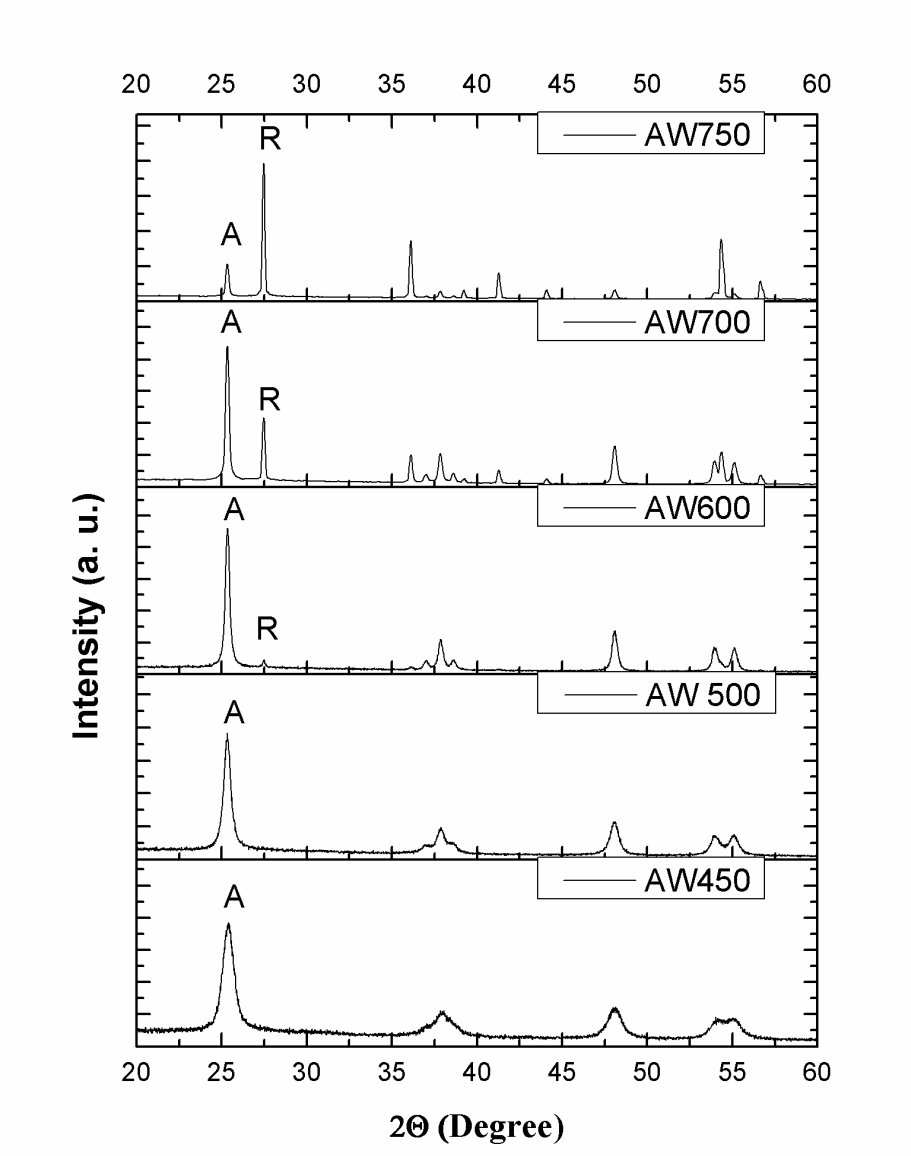

Figure 4. 2XRD pattern for alcohol washed samples calcined at different temperatures.

In all the calculations the value for k_A was 0.886 and for k_B 2.721, respectively. The weight percentage of different phases in the samples is mentioned in the Table 4.1. Broadening of peaks can be noticed at the low temperatures in the samples, is due to the 'nanostructuredness' of the samples.

The results for water washed samples (WW) indicate that the initial calcination involves the transformation of anatase in the starting material to brookite without formation of rutile (the brookite content increased from its initial content to 19.1% at 450° C and 19.6 % at 500°C). The peaks marked with letter 'B' corresponds to the 2θ = 30.830° (hkl – (211)) of the brookite.

Table 4. 1Phase composition and average crystallite size for different calcination temperatures.

	Samples Calcined at 450°C		Samples Calcined at 500°C		Samples Calcined at 600°C		Samples Calcined at 700°C		Samples Calcined at 750°C	
	WW	AW	WW	AW	WW	AW	WW	AW	WW	AW
Phase	A + B	A	A + B	A	A + B + R	A + R	A + R	A + R	R	A + R
$D_{avg(nm)}$	8.8	10.8	12.1	17	30.3	23.9	33.5	38.2	51.7	45.6
$W_{A\ (\%)}$	80.9	100	80.4	100	80.6	96.6	18.3	70.1	4.9	20.7
$W_{B\ (\%)}$	19.1	-	19.6	-	14.5	-	-	-		-
$W_{R\ (\%)}$	-	-	-	-	4.9	3.4	81.3	29.9	95.1	79.3

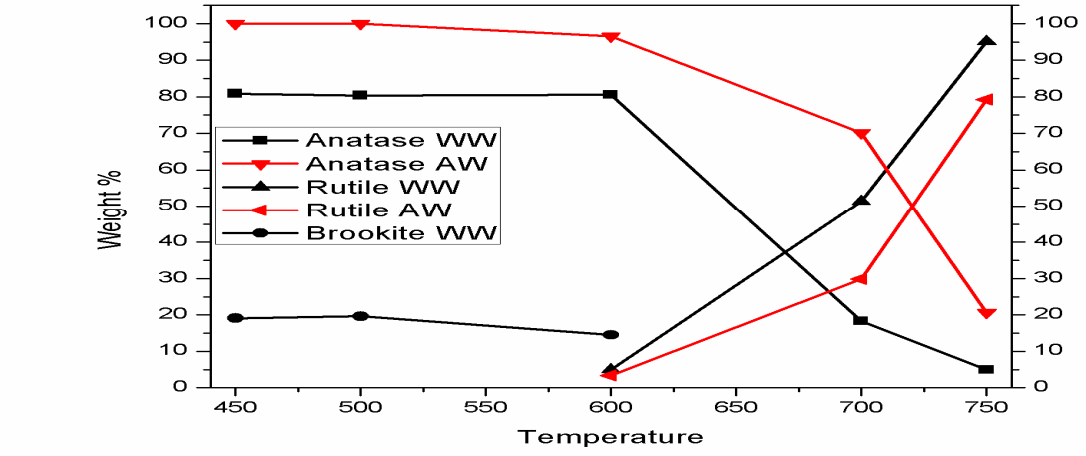

Figure 4. 3Change in weight percentage of different polymorphs with respect to temperature

Here also as expected, the crystalline phases grow with increasing calcination temperature. TiO_2 powders washed with water consist of a very small portion of brookite and

rutile phase along with the anatase as the major phase for calcination up to 600 ◦C. Titania washed with alcohol showed no sign of brookite, while starting to transform into rutile at 600°C.

The results for water washed samples (WW) indicate that the initial calcination involves the transformation of anatase in the starting material to brookite without formation of rutile (the brookite content increased from its initial content to 19.1% at 450° C and 19.6 % at 500°C). This is followed by a reaction of brookite to anatase at around 600° C as the small increase in the anatase amount can be noted. Upon heating, particles of brookite and anatase coarsen; however, the crystallite sizes of the two phases remain close in all calculations conducted at temperatures below 700°C as shown in the Table 4.2. Also almost complete transformation of anatase to rutile had taken place in the samples treated at 750°C. Transformation of anatase to brookite is a reversible transformation at lower temperature [51]. At higher temperature both brookite and anatase transforms directly to most stable form i.e. rutile. Transformation enthalpies of anatase-to-rutile and brookite-to-rutile reported by Mitsuhashi and Kleppa suggest that the thermodynamic phase stability for the three polymorphs is in the sequence of (rutile > brookite > anatase) [52]. Thus, anatase may either transform directly to rutile, or to brookite and then to rutile. Rutile rapidly increases in abundance as temperature increases above 700°C.

Table 4. 2Crystallite size (nm) of different polymorph present in the sample at different temperatures

	Crystallite size (nm)					
Calcination Temperature	Water Washed titania			Alcohol Washed titania		
	Anatase	Brookite	Rutile	Anatase	Brookite	Rutile
450° C	8.8	10.8	-	9.8	-	-
500° C	11.6	12.6	-	13.9	-	-
600° C	26.2	23.9	25.8	23.9	-	24.0
700° C	31.5	-	35.5	33.3	-	43.2
750° C	42.5	-	61.0	41.7	-	49.5

Similarly X-Ray patterns for the alcohol washed Titania are shown the figure 4.2. Alcohol washed samples were also calcined at the same temperature as that of water washed samples. Phases present in the samples calcined at different temperatures are marked with peaks present in the figure 4.2. Crystallite size, lattice parameters, d-spacings and weight percentage of the phases present were calculated in the same manner as mentioned above. In alcohol washed samples anatase can be seen as the major phase up to 700° C. Also, alike the water washed

samples; no brookite was identified in these samples. Also a considerable amount (i.e. 20.7 %) of anatase can be seen even at 750°C.

Earlier it had been reported that if particle sizes of the three nanocrystalline phases are equal, anatase is most thermodynamically stable at sizes less than 11 nm, brookite is most stable for crystal sizes between 11 and 35 nm, and rutile is most stable at sizes greater than 35 nm[53]. Also Kumar et al. reported in their study that alcohol washing of Titania prevent the anatase particles from reaching the critical nuclei size for transformation, by controlling packing and coordination of primary particles within the aggregates. It is the lower surface tension of alcohol which causes the prevention of aggregation of particles and produces loosely packed gel; whereas the higher surface tension of water during drying exerts higher inward drying stresses thus producing closed packed gel[54].

So from the above discussion it can be concluded that the dense particle coordination can be the reason for the anatase particles in the water washed samples to reach the stable particle size and transform into brookite at lower temperature as densely packed gels have lower activation energy for transformation. And loosely packed alcohol washed Titania thus avoids, the transformation to brookite at lower temperature.

The water washed gel transformed to rutile almost completely at 750°C where as one-fifth of the alcohol washed gel is still anatase. This may be due to following reasons:

1) In case of denser packed Titania (here it is water washed), the nucleation for transformation occurs at the interface and for loosely packed (i.e. alcohol washed), it occurs at both interface and surface (i.e. not attached to other particle). Activation energy for interface nucleation islower than that for surface nucleation [55]. For water washed samples more interface nucleation sites are present as compared to the interface nucleation sites in alcohol washed samples. Also the activation energy for the surface nucleation is high which is only achieved at high temperatures. So this can assumed as potential reason for relatively fast transformation in water washed gels.
2) The powders with larger volume fraction ofbrookite would have larger amount of nucleation sites as interface between brookite and anatase phase acts as a potential nucleation site and thus have higher reaction rate and lower transition temperatures. The existence of brookite,

therefore, is responsible for the enhancement of the Anatase to Rutile transition in case of water washed Titania [56].

3) Also comparatively larger particle size at 750° C can be seen in water washed Titania (refer table (4.5) which could be due to densely packed particle coordination. High degrees of packing had increased the number of particle-to-particle contact (coordination) in the dried gel, which would have led to the particle growth. As we heat treat as-prepared anatase, it would have converted to rutile only after growing to a certain size called the critical-nuclei-size. Lower packing density of alcohol-washed gels exhibit slower phase transformation and particle growth because particle to particle coordination is low, which enables the particle to grow to that critical size and thus restricting the phase transformation .

Above X-ray diffraction (XRD) patterns were recorded on a *XPERT-PRO diffractometer* under the following conditions: λ Cu K_α = 0.15406 nm, 40 mA, 45 kV, in the 20 - 60° (2θ) regions with scan step size of 0.0130° (along 2θ).

4.1. 2Thermal Analysis:

In figure 4.4 and 4.5, we can see the DSC - TG curve of water washed and alcohol washed samples respectively. In figure 4.4 the endothermic peak at 228° C represents the water loss from the very small pores present in the powder. Exothermic peaks at 409 °C and 693 °C represent the crystalline transformation and anatase-rutile transformation respectively.

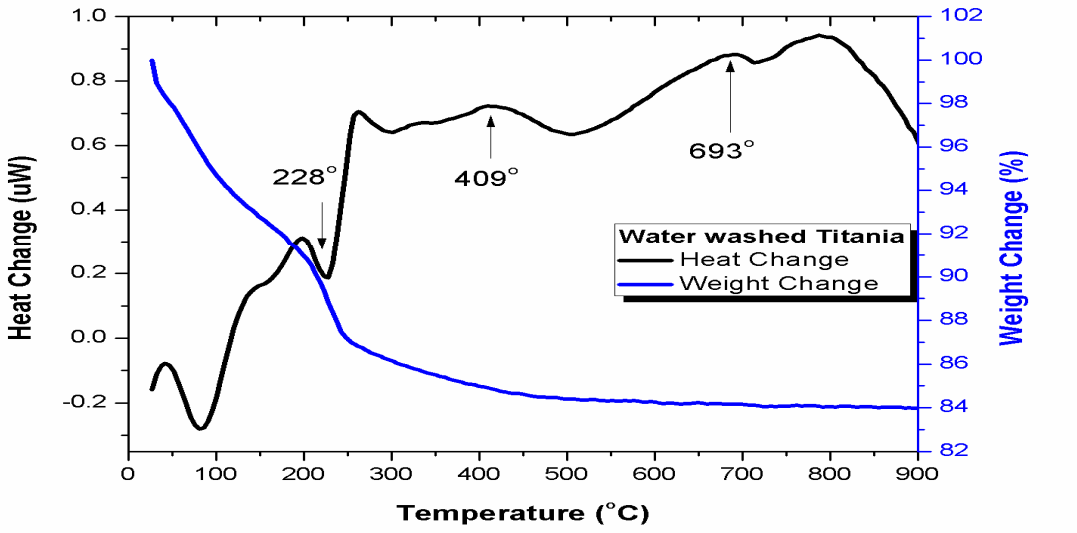

Figure 4.4 DSC-TG curve of water washed TiO_2 dried at 100°C.

Similarly in figure 4.5 peaks 448 °C and 777 °C gives the crystalline transformation and anatase-rutile transformation respectively for alcohol washed sample dried at 100 °C. Similar results have been previously reported by the other authors [54]. Also there a another peak after 780°C in figure 4.4 which can be ascribed to the exaggerated particle growth in the water washed samples.

Table 4.3Phase transformation temperatures obtained from DSC-TG curves.

Transformation	Water Washed Titania	Alcohol Washed Titania
Crystallization temperature (amorphous to anatase) (°C)	409	448
ART temperature (anatase to rutile) (°C)	693	777

TGA curve of the alcohol washed and water washed Titania samples show that alcohol washed samples undergo the net weight loss of 30 % whereas water washed samples had weight loss of 16 %. These results are matching with the TG analysis reported by **Kug Sug Hog** *et al.*[57]. This higher weight loss in alcohol washed Titania samples is due to the presence of larger amount of H_2O and OH than water washed samples even after the crystallization.

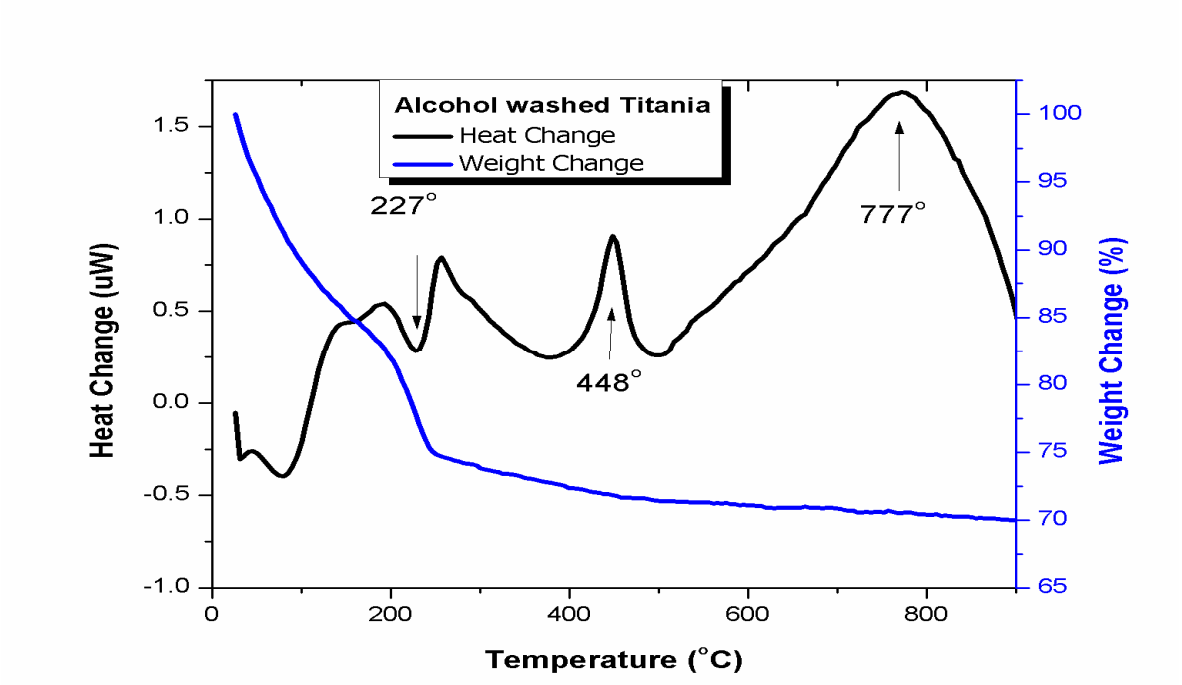

Figure 4.5DSC-TG curve of alcohol washed TiO_2 dried at 100°C.

4.1. 3UV-VIS Spectroscopy:

UV-vis - DRS spectra of catalysts were recorded on a UV-visible spectrophotometer (U-3900H Spectrophotometer) and ZnO was used as reference.

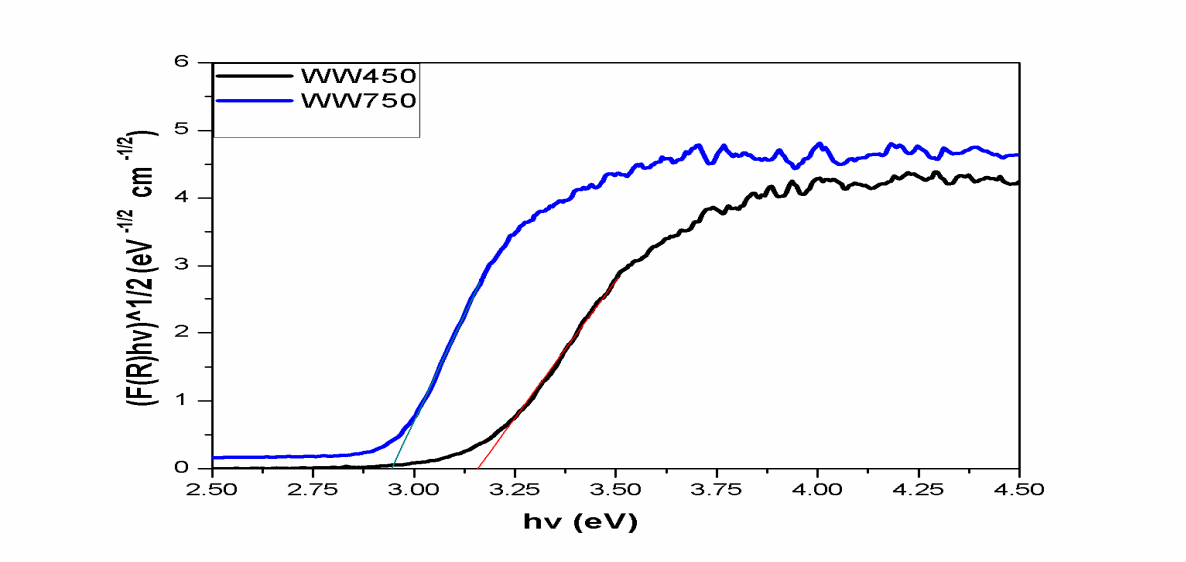

Figure 4.6UV–visible Diffused Reflectance spectra of water washed TiO_2

The UV-visible(DRS) spectra of the array of water washed and alcohol washed TiO_2 samples are shown in Figure 4.6 and 4.7 respectively. The sol-gel synthesized, water washed TiO_2 (WW450, WW500, WW600, WW700 and WW750) are characterized at about 392.6 nm, 394.8 nm, 412.0 nm, 387.6 nm and 421.0 nm (Eg ~ 3.15 eV, 3.14 eV, 3.00 eV, 2.94 eV and 2.94 eV,) respectively. Calculations were carried out using 'Kubelka – Munk' function.

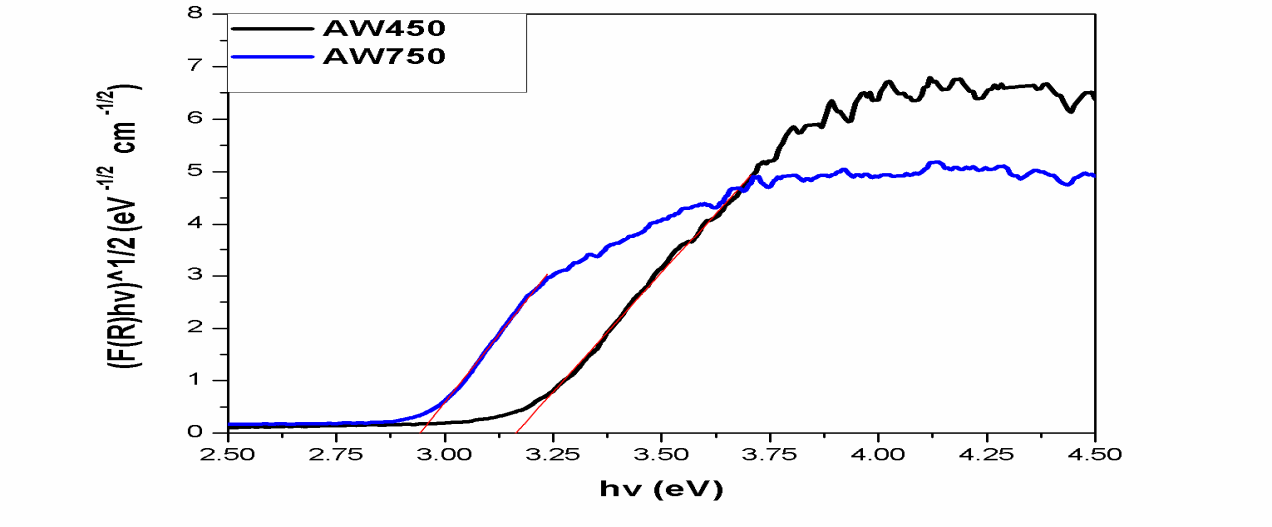

Figure 4.7 UV–visible Diffused Reflectance Spectra of Alcohol washed TiO_2

Similarly, alcohol washed TiO_2 (AW450, AW500, AW600, AW700 and AW750) shows reflectanceat about 392.1 nm, 394.3 nm, 382.7 nm, 421.0 nm and 421.4 nm (Eg ~ 3.16 eV, 3.15 eV, 3.14eV, 2.94 eV and 2.94 eV) respectively.

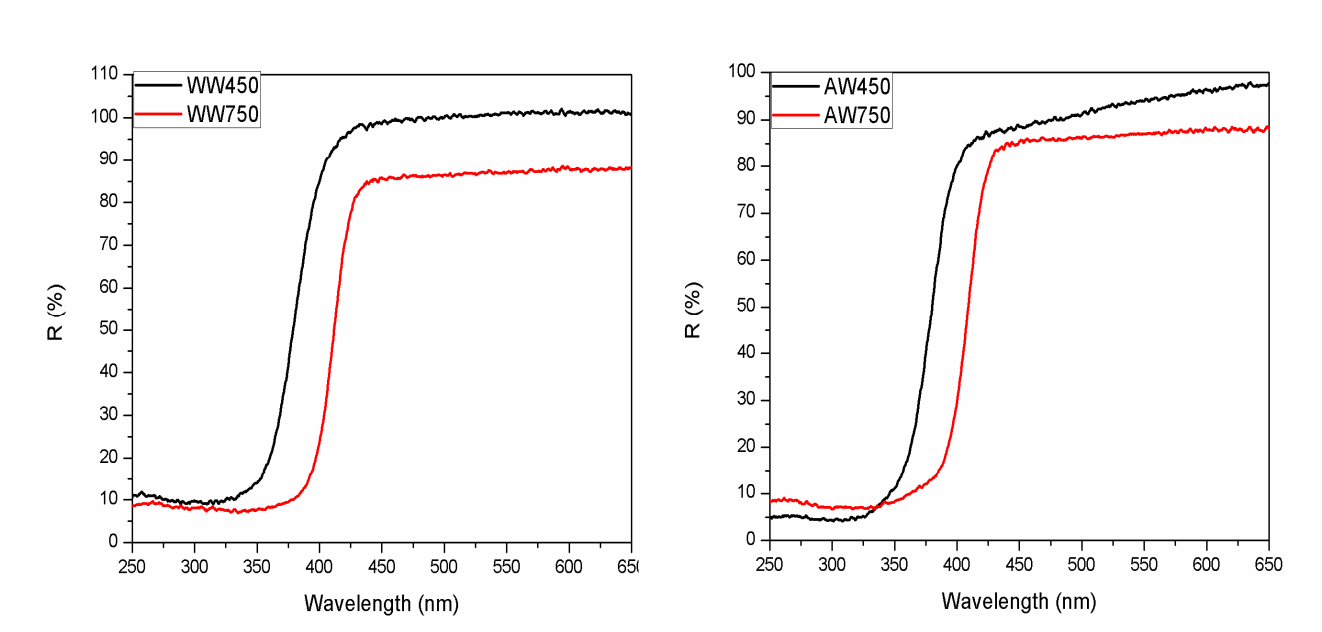

Figure 4. 8Reflection Spectra of Water washed (WW) Alcohol washed (AW) TiO_2

Table 4.4 Band gap, crystallite size and Rutile percentage present in the sample at different temperatures.

Calcination Temperature (° C)	Water Washed (WW)			Alcohol Washed (AW)		
	Band gap (eV)	Crystallite Size	Rutile %	Band gap (eV)	Crystallite Size	Rutile %
450	3.15	9	-	3.16	11	-
500	3.14	12	-	3.15	17	-
600	3.00	30	3.4	3.14	24	5
700	2.94	33	81	2.94	38	30
750	2.94	52	95	2.94	45	80

In both the figures with increase in calcination temperature decrease in the band gap energy can be observed. This could be due to following reasons:

1. From Table 4.4, it can be noted that with increase in the crystallite size (or particle size) a decrease in the band gap can be observed, which verified the quantum size effect on the band gap energy.
2. Also with increase in the rutile percentage in the samples, decrease in the band gap energy can be observed. This may be because; rutile and anatase have reported band gap energy of 3.0 eV and 3.2 eV respectively and with increase in the calcination temperature anatase rich samples transforms in to rutile and thus band gap shift accordingly [58].

4.1. 4FE-SEM:

Figure 4.9 shows the micrographs of Titania samples washed with water and alcohol calcined at 500 °C for 6 hours. Water washed samples show more densification as compared to alcohol washed samples. Also particle size for both the counterparts came up as similar. Average particle size was calculated using the software **AXIO VISION**, which comes out to be 37.0 nm and 35.3 nm for water washed and alcohol washed samples respectively. In the water washed sample micrograph some part showed densification with porosity on some other portion, whereas nearly homogeneous porosity can be seen in micrograph of alcohol washed samples.

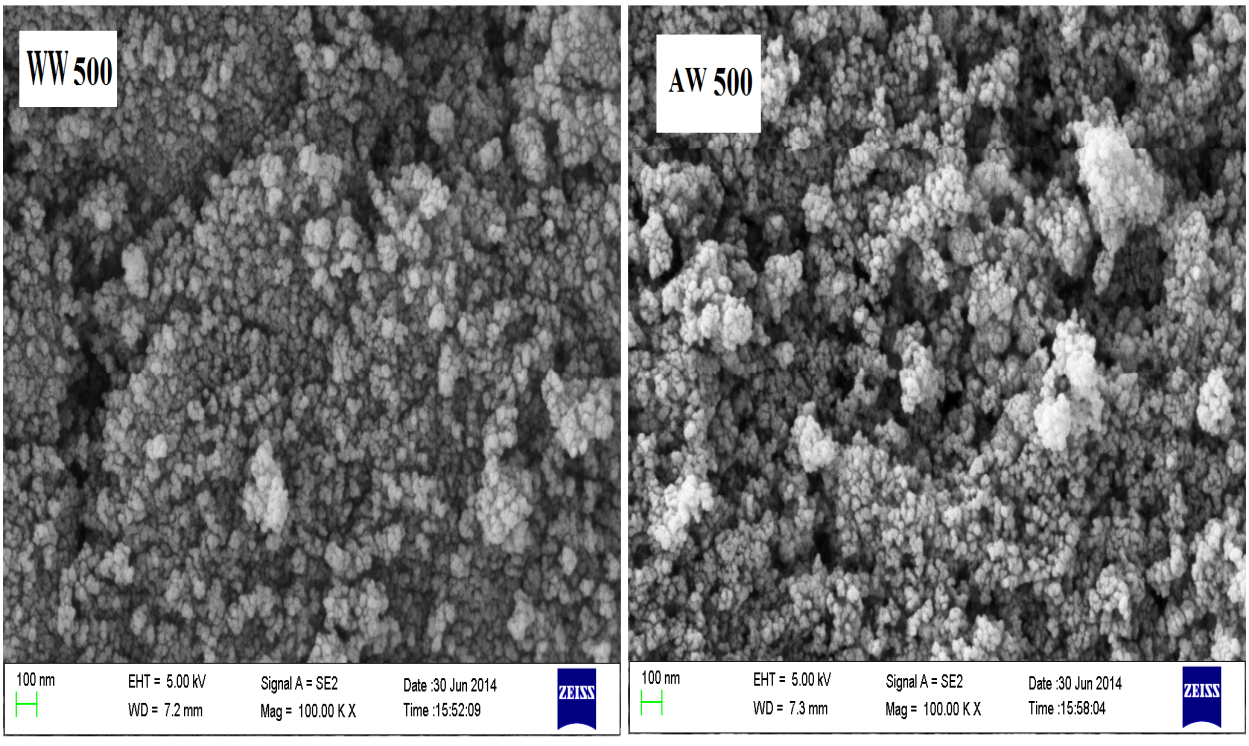

Figure 4. 9FE-SEM micrograph of water washed and Alcohol washed Titania heated at 500° C for 6 hours

Table 4.5 Particle size calculate from FE-SEM micrographs using software AXIO VISION

Water washed Titania		Alcohol washed Titania	
Sample	Particle size (nm)	Sample	Particle size (nm)
WW500	37.0	AW500	35.3
WW600	59.7	AW600	51.0
WW700	100.9	AW700	55.2
WW750	240.7	AW750	96.9

In the figure 4.10micrograph of Titania samples heated at 600° C for 6 hours can be seen. Completely dense (no porosity) water washed Titania can be observed in the figure. On the other hand porosity can be observed in the alcohol washed samples. Particle growth can be observed in the samples as the particle size increases to 59.7 nm and 51.0 nm for water washed and alcohol washed samples respectively.

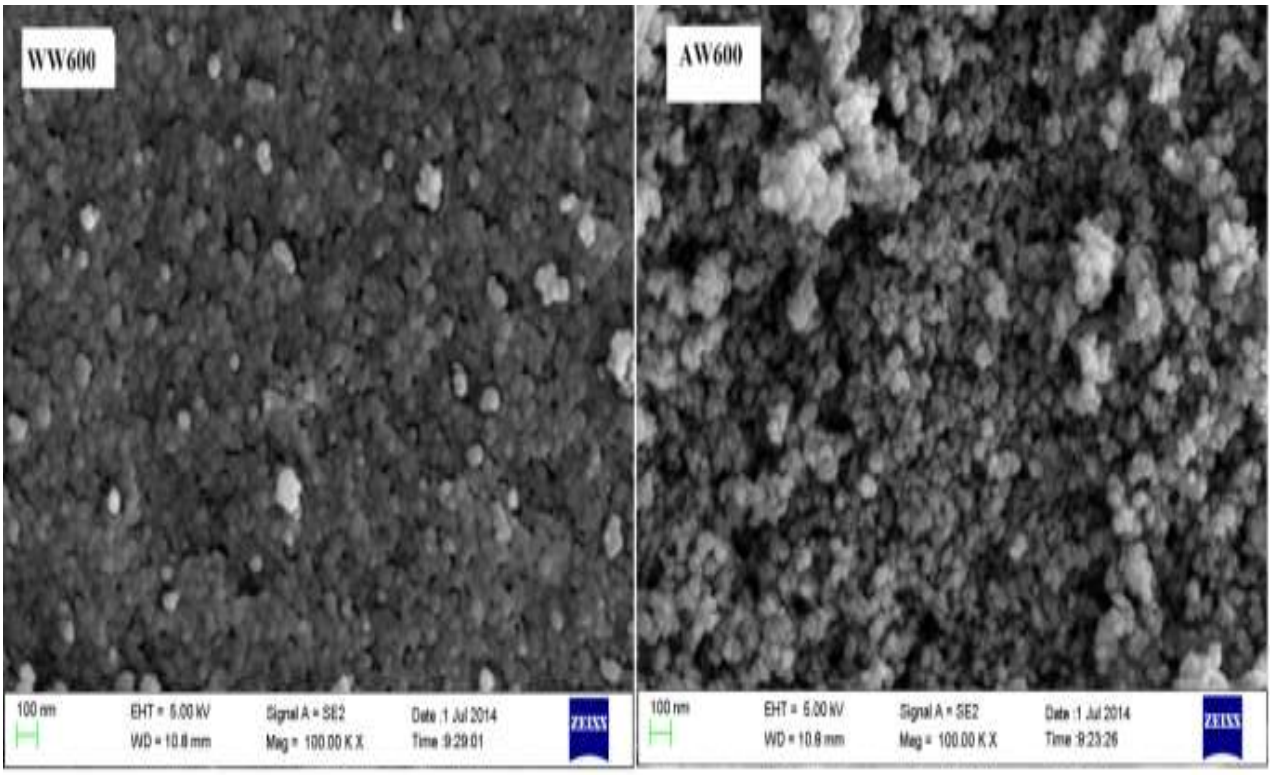

Figure 4.10FE-SEM micrograph of water washed and Alcohol washed Titania heated at 600° C for 6 hours

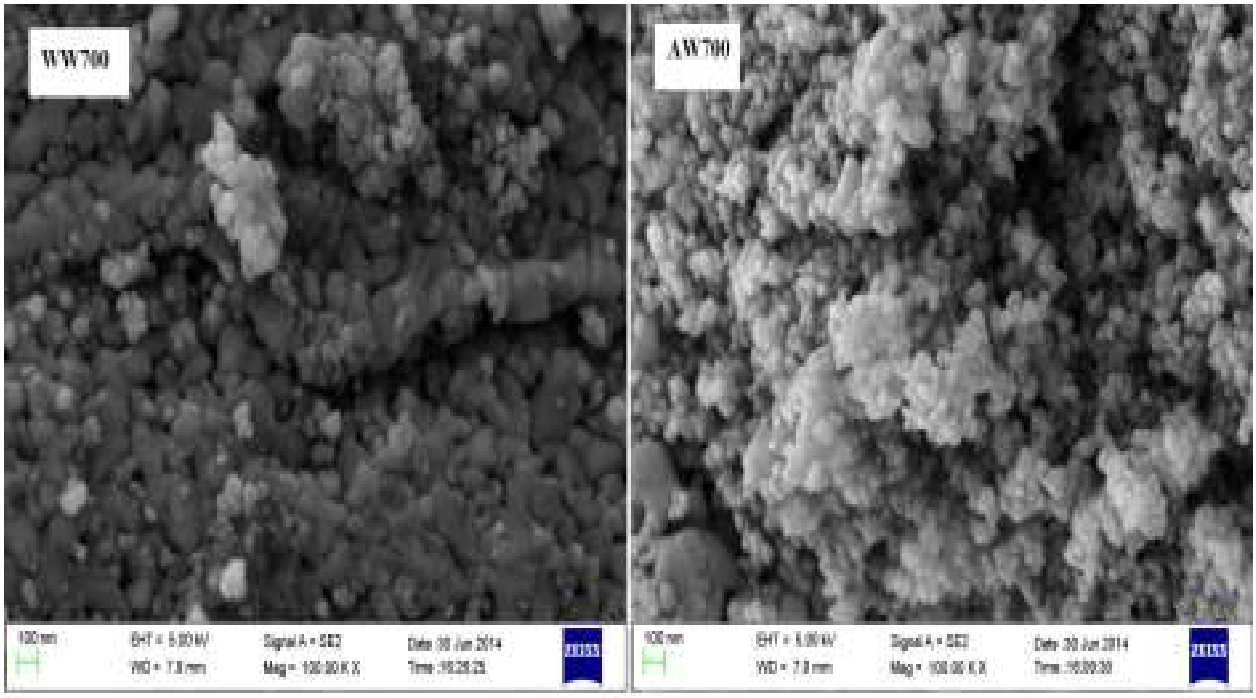

Figure 4. 11FE-SEM micrograph of water washed and Alcohol washed Titania heated at 700° C for 6 hours

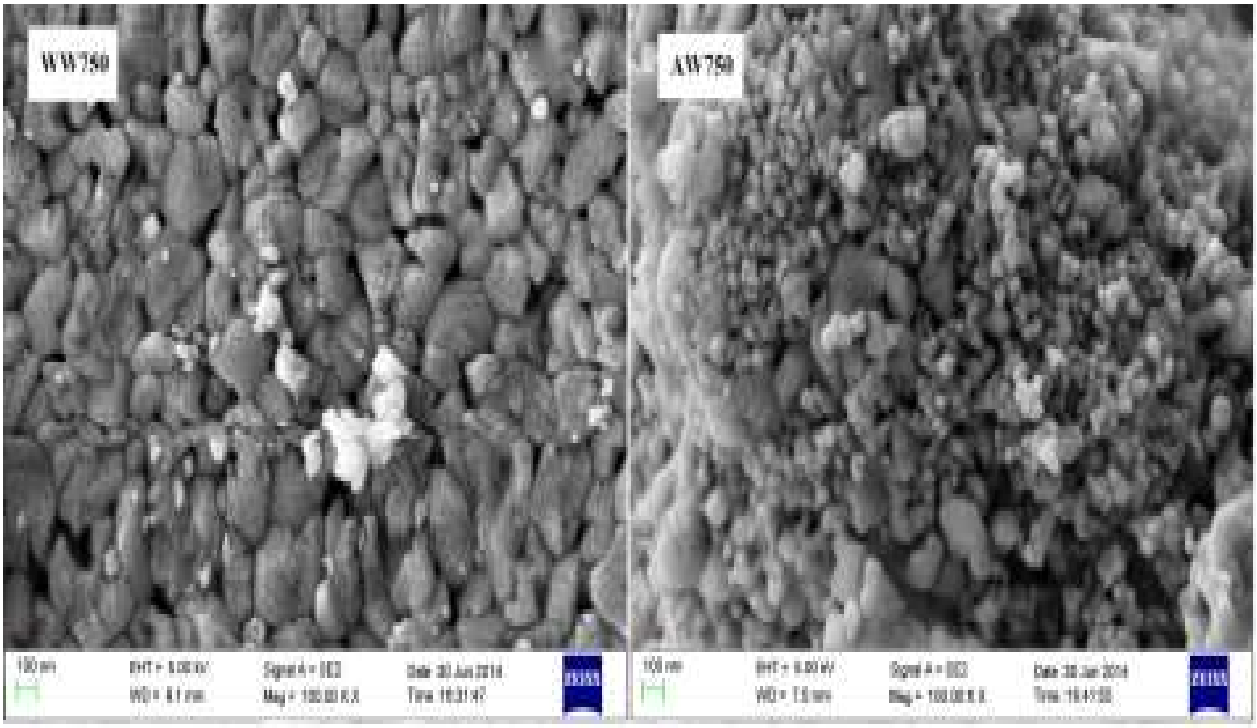

Figure 4. 12FE-SEM micrograph of water washed and Alcohol washed Titania heated at 750° C for 6 hours

Micrographs for the Titania samples heated at 700°C and 750°C can be seen in the figure 4.11 and 4.12 respectively. At both 700°C and 750°C water washed samples show densification

and the particle growth with particle size of 100.9 nm (at 700°C) and 240.7 nm (at 750° C). Whereas on the other hand in alcohol washed Titania micrographs porosity can be observed, with relatively lesser particle growth as compared to water washed samples.

4. 2Conclusions

In the summary of the report following things can be concluded:

- In water washed samples obtained after 450° C of calcination, brookite phase was identified by XRD, whereas no brookite formed in alcohol washed samples.
- ART temperature for alcohol washed samples is 777°C and 693°C for water washed samples. This behavior is due to replacement of water with 2-propanaol for Titania precipitates washing. 2-propanol has comparatively less surface tension, which helped in synthesizing gels with lower packing and water washed sample formed a dense gel. Dense gel (anatase) on heating will easily achieve the critical nuclei and transform to rutile rapidly than loosely packed gel.
- Porous structure is evident from the micrographs for the alcohol washed Titania even at 750°C, while completely dense (no porosity) is there in the water washed samples.
- At 750°C alcohol washed samples have particle size of 96 nm and water washed samples have 240 nm which could be due to the effect of particle-particle coordination.

4. 3 Future Scope

- Above synthesized powder can used as a catalyst to study their photocatalytic activity.
- Further effect of alcohol washing can be studied for doped titania.
- Other physical methods can also be employed for synthesizing thermally stable titania.

References

[1] Cristina B., Ivan P. and Kevin R., "Nanomaterials and Nanoparticles: Sources and Toxicity". *Biointersphases*; 2; 17; 2007.

[2] Debnath B., Shashank S., Niraj S., Ankesh K. and Seung-H. J.; "Nanotechnology, Big things from a Tiny World: a Review"; *International Journal of u- and e- Service, Science and Technology*; 2; 29; 2009.

[3] Muggli D. S. and Lefei D.; "Photocatalytic performance of sulfated TiO_2 and Degussa P-25 TiO_2 during oxidation of organics";*Applied catalysis B: Environmental*; 32; 181; 2001.

[4] Fujishima A.and HondaK.; "Electrochemical Photolysis of Water at a Semiconductor Electrode"; *Nature;* 238; 37; 1972.

[5] Xiaobo C. and Samuel M. S.; "Titanium dioxide nanomaterials: Synthesis, properties, modifications, and applications"; *Chemical Reviews*; 107; 2891; 2007.

[6] Linsebigler A. L., Lu G. and Yates J. T.; "Photocatalysis on TiO_2 surfaces: Principles, mechanisms, and selected results"; *Chemical Reviews*; 95; 735; 1995.

[7] Carp O., Huisman C.L., Reller A.; "Photoinduced reactivity of titanium dioxide"; *Progress in Solid State Chemistry*; 32; 33; 2004.

[8] Dorian A. H. H. and Charles C. S.; "Review of the anatase to rutile phase transformation"; *Journal of Materials Science*; 46; 855; 2011.

[9] Rothschild A., Levakov A., Shapira Y., Ashkenasy N. and Komem Y.; "Surface photo voltage spectroscopy study of reduced and oxidized nanocrystalline TiO_2 films"; *Surface Science*; 532; 456; 2003.

[10] Lei Q. and Haifei Z.; "Controlled freezing and freeze drying: a versatile route for porous and micro / nano - structured materials"; *Journal of Chemical Technology and Biotechnology*; 86; 172; 2011.

[11] Gerhard P. and Peter R.; "Angle-Dependent Optical Effects Deriving from Submicron Structures of Films and Pigments"; *Chemical Reviews*; 99; 1963; 1999.

[12] Salvador A., Pascual-Martı M.C., Adell R., Requeni A. and March J.G.; "Analytical methodologies for atomic spectrometric determination of metallic oxides in UV sunscreen creams"; *Journal of Pharmaceutical and Biomedical Analysis;* 22; 301; 2000.

[13] Juergen H. B., Andrejs B. and Robert E. M.; "TiO_2 pigment technology: a review"; Progress in Organic Coatings**;** 20; 1005; 1992.

[14] Shuai Y., Wanhua C. and Shengshui H.; "Fabrication of TiO_2 nanoparticles / surfactant polymer complex film on glassy carbon electrode and its application to sensing trace dopamine"; *Materials Science and Engineering : C*; 25; 479; 2005.

[15] Fujishima A. and Honda K.; "Electrochemical Photolysis of Water at a Semiconductor Electrode"; *Nature;* 238; 37; 1972.

[16] Grätzel M.; "Photoelectrochemical cells"; *Nature*; 414; 338; 2001.

[17] Xiuzhen W., Guangfeng Z., Jinfeng F. and Jinyuan C.; "Synthesis, characterization, and photocatalysis of well-dispersible phase-pure anatase TiO_2 nanoparticles"; *International Journal of Photoenergy*; Article ID 726872; 2013.

[18] Doshi R. and Alcock C.B.; "Effect of surface area on CO oxidation by the perovskite catalysts $La_{1-x}Sr_xMO_{3-\delta}$ (M = Co, Cr)"; *Catalysis Letters*; 18; 337; 1993.

[19] Bing G., Hangyan S., Kangying S., Yaowu Z. and Wensheng N.; "The study of the relationship between pore structure and photocatalysis of mesoporous TiO_2"; *Journal of Chemical Sciences*; 121; 317; 2009.

[20] Florence B., Patrick L. D. and Andre A.; "TiO_2 anatase-based membranes with hierarchical porosity and photocatalytic properties"; *Journal of Colloid and Interface Science*; 304; 545; 2006.

[21] Shannon, R. D. and Joseph A. P., "Kinetics of the Anatase-Rutile Transformation," Journal of the American Ceramic Society; 48; 391; 1965.

[22] Mackenzie K. J. D.; "The Calcination of Titania: The Effect of Additives on the Anatase-Rutile Transformation"; *Transactions and Journal of the British Ceramic Society*; 74; 29; 1975.

[23] Rao C., Turner A., and Honig J.; "Some Observations Concerning the Effect of Impurities on the Anatase-Rutile Transition," *Journal of Physics and Chemistry of Solids*; 11; 173; 1959.

[24] Banfield J. F.; Bishoff B. L; and Marc A. A.; "TiO_2 accessory minerals: coarsening, and transformation kinetics in pure and doped synthetic nanocrystalline materials," *Chemical Geology;* 110; 211; 1993.

[25] Gamboa J. A. and Daniel M. P.; "Effect of Chlorine atmosphere on the Anatase-Rutile transformation" *Journal of the American Ceramic Society*; 75; 2934; 1992.

[26] Wilska S. "An X-Ray Diffraction Study to Determine the Effect of the Method of Preparation Upon the Crystal Structure of TiO_2," *Acta Chemica Scandnavica*; 8; 1706; 1954.

[27] Garvie R.C.; "Stabilization of the Tetragonal Structure in Zirconia Microcrystals;" *The Journal of Physical Chemistry;* 82; 1978.

[28] Czanderna A.W., Rao C. N. R. and Honi J.M.; "The anatase-rutile transition Part l -Kinetics of the transformation of pure anatase"; *Transactions of the Faraday Society*; **54**; 1069; 1958.

[29] Meagher E. P. and George A. L.; "Polyhedral thermal expansion in the TiO_2, polymorphs: refinement of the crystal structures of rutile and brookite at high temperature"; *Canadian Mineralogist*; 17; 77; 1979.

[30] Mitsuhashi T. and Kleppa O.J.; **"**Transformation Enthalpies of the TiO_2 Polymorphs**";***Journal of American Ceramic Society*; 62; 356; 1979.

[31] Kumar K.N.P., Keizer K. and Burggraaf A.J.; "Textural stability of Titania- Alumina composite membrane"; *Journal of Materials Chemistry*; 3; 917; 1993.

[32] Kumar K.N.P., Keizer K. and Burggraaf A.J.; "Textural evolution and phase transformation in Titania membranes: Part 1. – Unsupported membranes"; *Journal of Materials Chemistry*; 3; 1141; 1993.

[33] Kumar K.N.P., Keizer K. and Burggraaf A.J.; "Textural evolution and phase transformation in Titania membranes: Part 2. – Supported membranes"; *Journal of Materials Chemistry*; 3; 1141; 1993.

[34] Kumar K.N.P; "Growth of rutile crystallites during the initial stage of anatase to rutile transformation in pure Titania and in titania- alumina composites"; *Scripta metallurgica et materialia*; 32; 873; 1995.

[35] Kumar K.N.P., Engell J., Keizer K., Okubo T. and Sadakata M.; "Pore-structure stabilization by controlling particle coordination"; *Journal of Materials Science Letters*; 14; 1784; 1995.

[36] Kumar P.N.K., Fujio M., Okubo T., Jalajakumari N., Keizer K., and Burggraaf A.J.; "High-temperature catalyst supports and ceramic membranes: Metastability and Particle Packing"; *Ceramics Processing*; 43; 2710; 1997.

[37] Hyuk J. Y., Pyung S. H., Hyun S. J., Kug S. H., Yong H. P., and Kyung H. K.; " Alcohol rinsing and crystallization behavior of precipitated Titanium Oxide"; *Journal of Colloid and Interface Science*; 211; 321; 1999.

[38] Zhang H. and Banfield J. F.; "Understanding polymorphic phase transformation Behavior during growth of nanocrystalline aggregates: Insights from TiO_2"; *Journal of Physical Chemistry B*; 104; 3481; 2000.

[39] Gonghu L., Dimitrijevic M. N., Le C., Jamie M. N., Tijana R., and Gray K. A.; "The important role of tetrahedral Ti^{4+} sites in the phase transformation and photocatalytic activity of TiO_2 nanocomposites"; *Journal of American Chemical Society*; 130; 5402; 2008.

[40] Kumar K. N. P., Izutsu H., Fray D. J., Yves C., Tatsuya O.; "Alcohol washing as a way to stabilize the anatase phase of nanostructured titania through controlling particle packing"; *Journal of Materials Science;* 44; 5944; 2009.

[41] Suminto W., Mukti R. R., Kumar N. P. K., Wang J., Wilfried W. and Okubo T.; "Critical Nuclei Size, Initial Particle Size and Packing Effect on the Phase Stability of Sol-Peptization-Gel-Derived Nanostructured Titania"; *Langmuir*; 26; 4567; 2010.

[42] Barbara G., Marta G., Bogumił K. and Lubkowski K.; "Study of the anatase to rutile transformation kinetics of the modified TiO_2"; *Polish Journal of Chemical Technology*; 15; 73; 2013.

[43] Carlo R. P., Carlo M. C., Luigi S., Marcello S., Alberto C., Stefano E., and Francesco D.; "Anatase-to-Rutile Phase Transition in TiO_2 Nanoparticles Irradiated by Visible Light"; *The Journal of Physical Chemistry: C*; 17 ; 7850; 2013.

[44] Mattsson A., Christian L., Snejana B., Vaclav S. and Osterlund L.; "Characterization, phase stability and surface chemical properties of photocatalytic active Zr and Y co-doped anatase TiO_2 nanoparticles"; *Journal of Solid State Chemistry* ; 199; 212 ; 2013.

[45] Noguchi D., Yukie H., Tomohiro E., Kazuya K., Shoji F., Yoshihiko K., Fumihiro S. and Ichiro S.; "Structural control and photocatalytic properties of photocatalytic TiO_2 thin films prepared using two-step deposition including radical-assisted sputtering"; *Japanese Journal of Applied Physics*; 53; 065501 ;2014.

[46] Wang J., Hui L., Hongyi L., Chen Z., Hong W., and Dasheng L.; "Mesoporous TiO_2 thin films exhibiting enhanced thermal stability and controllable pore size: Preparation and photocatalyzed destruction of cationic dyes"; *Applied Materials and Interfaces*; 6; 1623; 2014.

[47] Brinker W. and Scherer G. W.; "Sol–gel science, the physics and chemistry of sol–gel processing"; *Academic Press, Boston*; 14; 908; 1990.

[48] Brinker C. J., Hurd A. J., Schunk P. R. , Frye G. C. and Ashley C.S.; "Review of sol-gel thin film formation"; *Journal of Non-Crystalline Solids*; 147; 3093; 1992.

[49] Ulrich S.; "Chemical modification of titanium alkoxides for sol–gel processing"; *Journal of Materials Chemistry*; 15, 3701; 2005.

[50] Doeuff S., Henry, Sanchez C. and Livage J. "Hydrolysis of titanium alkoxides: Modification of the molecular precursor by acetic acid"; *Journal of Non-Crystalline Solids;* 89; 3039; 1987.

[51] Masih R., Seyyed M. M. K. and Kun H. L.; "The role of brookite in mechanical activation of anatase-to-rutile transformation of nanocrystalline TiO_2: An XRD and Raman spectroscopy investigation"; *CrystEngComm*; 13; 5055; 2011.

[52] MitsuhashiT. and Kleppa O. J.; "Transformation enthalpies of the TiO_2 polymorphs"; *Journal of the American Ceramic Society;* 62; 356; 1979.

[53] Zhang H. and Banfield J. F.; "Understanding polymorphic phase transformation Behavior during growth of nanocrystalline aggregates: Insights from TiO_2"; *Journal of Physical Chemistry B*; 104; 3481; 2000.

[54] Kumar K.N.P., Izutsu H., Fray D.J., Yves C., Tatsuya O.; "Alcohol washing as a way to stabilize the anatase phase of nanostructured titania through controlling particle packing"; *Journal of Materials Science*; 44; 5944; 2009.

[55] Zhang H. and Banfield J. F.; "Phase transformation of nanocrystalline anatase-to-rutile via combined interface and surface nucleation"; *Journal of Materials Research*; 15; 437; 2000.

[56] Hu Y., Tsai H. L., Huang C. L.; "Effect of brookite phase on the anatase–rutile transition in titania nanoparticles"; *Journal of the European Ceramic Society*; 23; 691; 2003.

[57] Hyuk J.Y., Pyung S.H., Hyun S.J., Kug S.H., Yong H.P., and Kyung H.K.; "Anatase–Rutile Transition of Precipitated TitaniumOxide with Alcohol Rinsing"; *Journal of Colloid and Interface Science*; 223; 16; 2000.

[58] Lee H.S., Woo C.S., Youn B.K., Kim S.Y., Oh S.T., Sung Y.E., and Lee H.I.; "Bandgap modulation of TiO_2 and its effect on the activity in photocatalytic oxidation of 2-isopropyl-6-methyl-4-pyrimidinol"; *Topics in Catalysis*; 35; 3; 2005.